Journal of Statistical Physics, Vol. 72, Nos. 3/4, 1993

Critical Dynamics of the Three-Dimensional Ising Model: A Monte Carlo Study

Hans-Otto Heuer[1]

Received November 4, 1992; final March 10, 1993

Extensive Monte Carlo simulations have been performed to analyze the dynamical behavior of the three-dimensional Ising model with local dynamics. We have studied the equilibrium correlation functions and the power spectral densities of odd and even observables. The exponential relaxation times have been calculated in the asymptotic one-exponential time region. We find that the critical exponent $z = 2.09 \pm 0.02$ characterizes the algebraic divergence with lattice size for all observables. The influence of scaling corrections has been analyzed. We have determined integrated relaxation times as well. Their dynamical exponent z_{int} agrees with z for correlations of the magnetization and its absolute value, but it is different for energy correlations. We have applied a scaling method to analyze the behavior of the correlation functions. This method verifies excellent scaling behavior and yields a dynamical exponent z_{scal} which perfectly agrees with z.

KEY WORDS: Ising model; dynamics; Monte Carlo simulations.

1. INTRODUCTION

Critical phenomena are characterized by a dramatic increase of the correlation length and of the relaxation time of a system. Both the characteristic length scale and time scale diverge at the critical point. This phenomenon has been the subject of intensive theoretical and experimental research for a long time. By renormalization group (RG) methods it has been shown that the static critical behavior depends on only a few characteristics of the system, such as symmetry, dimension, and interaction type. RG approaches have led to universal properties, e.g., critical exponents, amplitude ratios, and scaling functions, which are in good accord with high-temperature expansions, Monte Carlo simulations, and experiments.

[1] Theoretische Physik III, Ruhr-Universität Bochum, Germany.

0022-4715/93/0800-0789$07.00/0

In analogy to static critical phenomena, scaling of dynamical properties was formulated at the very beginning of the renormalization group age.[1] It has been shown that the static universality classes are not the same as the dynamic ones.[2] The latter depend on the conservation laws and on the coupling of the system to additional degrees of freedom and their conservation laws. The quantity of central interest is the dynamical exponent z which describes the scaling behavior, $\chi(q, \omega) = q^{-(2-\eta+z)}\chi_0(\omega q^{-z})$, of correlation functions at the critical point of the infinite system.[2] Dynamical finite-size scaling leads to the divergence $\tau(L) \sim L^z$ of the asymptotic relaxation time of finite lattices.[3,4] The integrated relaxation time for a given observable $\mathscr{A}$ is an integral measure of all relaxation processes of the system weighted according to their contributions to $\mathscr{A}$. It diverges with an exponent $z_{\text{int},\mathscr{A}}$, leading to increasing computing times at the critical point.[5]

In this paper, we are concerned with the local dynamics of the three-dimensional Ising model at its critical point. This dynamics corresponds to the model A type (no conservation laws)[2] and has been treated in a large number of papers. The corresponding time-dependent Ginzburg–Landau–Wilson (GLW) model has been studied by RG methods. A perturbation expansion has been performed around the critical dimension $d_c = 4$ in $\varepsilon = d_c - d$ and in $1/n$, respectively, where n is the spin dimension. Above the critical dimension $d_c = 4$, one finds conventional van Hove theory with $z = 2 - \eta = 2$. Below d_c, the perturbation expansion leads only to tiny corrections which depend on the spin dimension n, on the order in ε, and on the parametric form that is evaluated from the ε-expansion.[6] For Ising systems ($n = 1$), the form $z = 2 - \eta + \Delta^*$ extrapolates to $z = 1.995$, using the best result[6] $\Delta^* = 0.032(1 - 0.216\varepsilon) + O(\varepsilon^4)$ and $\eta = 0.03$ in $d = 3$ dimensions.[7] Using the parametrization $z = 2 - c\eta$ with $c = 0.07261(1 - 1.687\varepsilon) + O(\varepsilon^2)$,[6] one obtains $z = 1.984$ in $d = 3$. In a later work about interface fluctuations in Ising systems, a critical exponent $z = 2 + \varepsilon' - \varepsilon'^2 + O(\varepsilon'^3)$ was derived by expansion around $d_c = 1$ ($\varepsilon' = d - 1$).[8] A tentative interpolation of this result with the expansion around $d_c = 4$ leads to $z = 2.017$.

A distinctly different conclusion was obtained by a high-temperature expansion of the simple cubic Ising model with Glauber dynamics. Based on the magnetization-correlation function, the relaxation time was shown to diverge as $\tau \sim \varepsilon^{-\nu z}$ with $\nu z = 1.40$ near the critical point ($\varepsilon = T/T_c - 1$). With the static exponent $\nu = 0.63$, one obtains $z = 2.22$.[9]

A geometric approach to critical dynamics has recently been proposed[10,11] which is based on the description of critical properties by Fortuin–Kasteleyn clusters.[12] The assumption of stepwise growth and the contraction of these clusters links dynamic properties with static ones and

with the geometric properties of clusters. In a Flory-like approximation, the dynamic critical exponents $z = 2.14$ and $z = 2.05$ have been calculated in $d = 2$ and $d = 3$ dimensions, respectively. The critical dynamics has been studied by Monte Carlo simulations in various ways. In a simulation of large lattices up to 360^3, the exponent Δ' of the nonlinear relaxation time was determined, leading to $z = 2.17 \pm 0.06$ via the relation $\Delta' = \Delta + \beta$.[13] Dynamic Monte Carlo renormalization group methods were used thereafter. Their estimates of the critical exponent were $z = 2.11 \pm 0.03$[14] (nonlinear relaxation time, maximum size $L = 128$) and $z = 2.08$[4] (linear relaxation time, $L = 16$). Extension of the first work to extremely large lattices led to the lower but less precise value of $z = 1.95 \pm 0.1$.[15] The latest high-powered Monte Carlo works have measured the equilibrium dynamics at the critical point. A simulation on a special-purpose machine[16] was performed with an investment of 1.2×10^{14} single spin flips. An exponent $z = 1.99 \pm 0.02$ was calculated from lattice sizes $L = 24$, 40, and 64. Unfortunately, there is some suspicion that the random number generator is not as perfect as it should be.[17, 18] The method of damage spreading has been applied recently to heat-bath dynamics using lattice sizes up to 51^3, leading to $z = 2.02 \pm 0.03$.[19] The latest Monte Carlo work has invested about 5×10^{12} single spin updates.[20] A critical exponent $z = 2.04 \pm 0.03$ was obtained from magnetization correlations and a compatible, but less precise value from energy correlations.

It is obviously not possible to draw a final conclusion about the true dynamical exponent z of the three-dimensional Ising model with local dynamics. Although there appears to be a convergence to the RG estimate $z = 2.02$ in recent years, there are severe discrepancies among analytical as well as numerical results. In two dimensions, the dynamical exponent $z_{2D} \simeq 2.14$ seemed to be "accepted" for a long time. A recent damage spreading study[21] has led to the conclusion that the slowest modes relax with an exponent z larger than 2.27. Concluding, one may state that different methods, different observables, and different computing efforts have led to diverse results. Apart from these technical aspects, a valid comparison of simulations and renormalization group results necessitates the inclusion of correction-to-scaling terms. This has not even been attempted in the past. Claimed error bars on estimates of z which take into account only *statistical* errors have to be viewed with caution. This will be demonstrated explicitly in this paper.[2]

[2] During the revision of this paper, preliminary results of our analysis were published in a short form as ref. 22. These results shattered the consensus about the dynamic exponent z and motivated further investigations leading to $z = 2.10 \pm 0.04$[23] and $z = 2.06 \pm 0.02$.[24] Large lattices up to 1536^3 have been simulated and the exponent z has been fitted from the nonequilibrium relaxation of the magnetization.

Here, we present the results of a large-scale simulation of the equilibrium dynamics of the three-dimensional Ising model. An investment of 1.3×10^{13} single spin flips has been made and a thorough finite-size scaling analysis has been performed. In Section 2 we briefly describe the model, introduce the notation, and summarize technical details of the simulation. Monte Carlo estimators of correlation functions and power spectral densities are discussed in Section 3. Their statistical and systematic errors are calculated and compared to our data. In Section 4 we discuss the time and frequency dependences of the correlation function and of the power spectral density, respectively. A bulk region and a finite-size region must be distinguished for a proper determination of the asymptotic relaxation time. Section 5 contains a discussion of odd and even observables of the Ising model with emphasis on their qualitatively different behavior. Section 6 treats the analysis of integrated and exponential relaxation times. The dynamical exponents $z_{\mathscr{A}}$ and $z_{\text{int},\mathscr{A}}$ of exponential and integrated relaxation times are determined for three observables. We find good agreement of all estimates $z_{\mathscr{A}}$, but a significant deviation from the renormalization group value for $d=3$ dimensions. The influence of scaling corrections is discussed in view of this discrepancy. We find that the dynamical exponent $z_{\text{int},\mathscr{A}}$ of the magnetization $\mathscr{M}$ and its absolute value $|\mathscr{M}|$ agrees surprisingly well with our exponent z. Energy correlations are more strongly influenced by short time scales, leading to a different exponent $z_{\text{int},\mathscr{E}}$. As our third method of analysis, we investigate the scaling behavior of the correlation functions in Section 7. This method does not make any assumption about the time dependence, but simply collapses all data by the hypothesis of scaling. We find excellent scaling behavior and an exponent z_{scal} which agrees very well with z. Section 8 summarizes our results and gives an outlook to future work.

2. NOTATIONS

We investigate the three-dimensional Ising model on a simple cubic lattice defined by

$$\mathscr{H} = -J \sum_{\langle ij \rangle} S_i S_j - H \sum_i S_i \tag{1}$$

where the sum is over all nearest neighbor pairs; a magnetic field H may couple to each spin $S_i = \pm 1$; here we set $H \equiv 0$. The coupling constant is $J \equiv 1$ henceforth, i.e., we measure temperatures in units of J/k_B (k_B is Boltzmann's constant). The Ising model shows a spontaneous symmetry breaking at its critical temperature $T_c = 4.51154$.[25–27] The theoretical

understanding of the static critical properties is excellent; RG results[7] agree very well with high-temperature expansions[28] and with Monte Carlo results.[25–27]

We define thermodynamic quantities such as the magnetization M and the energy E as densities, normalized to the number of spins in the system. The canonical ensemble average is denoted by

$$\langle \mathscr{A} \rangle = \sum_{\mathscr{S}} \pi(\mathscr{S})\, \mathscr{A}(\mathscr{S}) \tag{2}$$

where $\mathscr{S} \equiv \{S_i\}$ is a short-hand notation for the microstate of the system and $\mathscr{A}$ is an observable of the system (functional of the microstate $\mathscr{S}$). Since we simulate finite lattices of size L^d, the state space $\mathscr{Q} = \{\mathscr{S}_i\}$ is large ($\dim \mathscr{Q} = 2^{L^d}$), but finite. The canonical probability distribution in (2) is defined by

$$\pi(\mathscr{S}) = \frac{1}{Z} \exp[-\beta \mathscr{H}(\mathscr{S})] \tag{3}$$

where $\beta \equiv 1/T$ and Z is the partition function. In order to distinguish properly between observables $\mathscr{A}$ which are random numbers and thermodynamic quantities $A = \langle \mathscr{A} \rangle$ in (2) which are averages of observables, we use the script notation for observables. Thus, the observable of the magnetization is denoted as

$$\mathscr{M} = \frac{1}{N} \sum_i S_i \tag{4}$$

and the observable of the energy is

$$\mathscr{E} = \frac{1}{N} \sum_{\langle ij \rangle} S_i S_j \tag{5}$$

In Monte Carlo simulations the canonical average is estimated by the time average over a finite Markov chain of microstates $\mathscr{S}(t)$ which obeys the master equation

$$\frac{dP_i}{dt} = \sum_j [P_j p_{ji} - P_i p_{ij}] \tag{6}$$

We refer to the standard literature about Markov chains[29–31] and the Monte Carlo method[32, 33] for details concerning the conditions that have to be fulfilled by the transition matrix p_{ij} of (6) to ensure convergence of the probability vector $P(\mathscr{S}_j) \equiv P_j$ to the canonical probability $\pi(\mathscr{S}_j)$ of (2).

In this paper we choose the Metropolis transition probability

$$p_{ij} = \mathrm{Min}\{1, \exp[-\beta(\mathscr{E}_j - \mathscr{E}_i)]\} \tag{7}$$

to simulate local dynamics without conserved quantities. Here $\mathscr{E}_i$ and $\mathscr{E}_j$ are the energy observables of the initial state $\mathscr{S}_i$ and of the new microstate $\mathscr{S}_j$, respectively. The probability (7) is compared to a random number. We use the Kirkpatrick–Stoll random number generator[34] with the trinomial ($p = 250$, $q = 147$) and a careful initialization procedure. The dynamics defined by Eqs. (6) and (7) can be written in short-hand notation as

$$\frac{dP}{dt} = \mathscr{L}P \tag{8}$$

where $\mathscr{L}$ is the Liouville operator.

The definition of p_{ij} in (7) has to be supplemented by the prescription for how to move through the lattice and change spins. As usual in vectorized algorithms, the whole lattice is divided into two interpenetrating sublattices and the spins are changed sequentially in each sublattice. We use periodic-helical boundary conditions for favorable vectorization. It is generally assumed that the type of dynamics (Metropolis, Glauber, heat-bath) as well as the boundary conditions and the way one moves through the lattice belong to the irrelevant properties of the model. However, the absolute values of relaxation times and the magnitude of finite-size corrections may depend on these details.

The time average of an observable $\mathscr{A}$ over the discrete time series $\{\mathscr{A}(t)\}$ is denoted by an overbar,

$$\bar{\mathscr{A}} = \frac{1}{n}\sum_{i}^{n} \mathscr{A}(i) \tag{9}$$

to distinguish it from the canonical average $\langle \mathscr{A} \rangle$ of (2) to be estimated. We thermalize the system over long periods with $n_0 \geqslant 20\tau_{\exp,\mathscr{A}}$ Monte Carlo steps per spin[33] to achieve thermal equilibrium. This has been checked after the first approximate values of $\tau_{\exp,\mathscr{A}}$ have been calculated from preliminary rums. Summations over time series are understood to exclude the thermalization. The actual run lengths for the calculation of time averages vary between 10^6 and 3×10^6 MCS/spin, depending on the lattice size. We perform several runs with different random number streams. The details of the simulation of each lattice size L are summarized in Table I. We point out that the distribution of statistical weight $g(L)$ corresponds to a nearly optimal distribution in the sense of ref. 35.[3]

[3] Numerical data obtained by extensive and "expensive" simulations should be made available to others. If the reader wishes to apply his or her own techniques of data analysis, the author offers to distribute his raw data by e-mail.

Table I. Distribution of Computing Time on Lattice Size L^a

L	n_{run}	$n_{\text{upd}} \cdot 10^{-6}$	$n_{\text{tot}} \cdot 10^{-6}$	$m_{\mathscr{M}} \cdot 10^{-3}$	$m_{\mathscr{E}} \cdot 10^{-3}$
20	8	0.78	6.2	115	176
26	12	1.08	13.0	137	222
30	6	2.7	16.2	129	215
36	14	1.57	22.0	118	205
40	9	2.7	24.3	105	180
46	8	2.7	21.6	70	126
50	7	2.7	18.9	51	91
60	8	2.7	22.0	41	75

[a] n_{run} is the number of different runs, each with the number n_{upd} of lattice updates given in the third column. The fourth column, n_{tot}, is the total amount of lattice updates invested on lattice size L. Here $m_{\mathscr{M}}$ and $m_{\mathscr{E}}$ are the numbers of effectively uncorrelated observables, according to Eq. (18), using our estimates $\hat{\tau}_{\text{int},\mathscr{A}}$ in Table III.

The Markov process defined by Eqs. (6) and (7) is a process in the state space $\mathscr{Q}$ of microstates $\mathscr{S}$. Each observable $\mathscr{A}$ is a functional of $\mathscr{S}$ and projects dynamical properties of the system into the space of macroscopic observables. In the language of time-series analysis,[36] the series $\mathscr{A}(t)$ itself is called a stationary stochastic process. Its dynamical properties are described by the autocorrelation function

$$\phi_{\mathscr{A}}(t) = \langle \mathscr{A}(s+t)\, \mathscr{A}(s) \rangle - \langle \mathscr{A} \rangle^2 \tag{10}$$

which depends only on the time difference t because of stationarity. We shall be mainly concerned with the normalized autocorrelation function defined as

$$\Phi_{\mathscr{A}}(t) = \frac{\phi_{\mathscr{A}}(t)}{\phi_{\mathscr{A}}(0)} \tag{11}$$

Under the usual conditions adopted above which ensure that the canonical distribution is the unique stationary distribution, one can write the autocorrelation function $\Phi_{\mathscr{A}}(t)$ in a spectral form[37] as

$$\Phi_{\mathscr{A}}(t) = \int_{-1}^{1} \lambda^{|t|}\, d\tilde{\rho}_{\mathscr{A}}(\lambda) \tag{12}$$

The measure $d\tilde{\rho}_{\mathscr{A}}(\lambda)$ depends explicitly on the observable $\mathscr{A}$. With the restriction to the usual case where only positive eigenvalues λ are relevant for dynamic critical behavior, we can write Eq. (12) as an integral over all relaxation times weighted with the measure $\rho_{\mathscr{A}}(\tau)$ as

$$\Phi_{\mathscr{A}}(t) = \int_{0}^{\infty} \exp(-|t|/\tau)\, d\rho_{\mathscr{A}}(\tau) \tag{13}$$

In this sense, each observable has its characteristic distribution $\rho_{\mathscr{A}}(\tau)$ of relaxation times τ, which are related to the eigenvalues λ of $\mathscr{L}$ in (8) by $\tau^{-1} = -\log|\lambda|$. If the state space $\mathscr{Q}$ is finite, then the measure $\tilde{\rho}_{\mathscr{A}}(\lambda)$ is supported on the interval $[-\lambda^*, +\lambda^*]$ with $\lambda^* < 1$.[37] In this case, the largest relaxation time is finite. If the state space $\mathscr{Q}$ is infinite, then λ^* may reach $\lambda^* = 1$, leading to the divergence of the largest relaxation time of the system. This situation is found at the critical point of the infinite system. Stationarity breaks down at this point.

Since the RG approach to dynamics[2] applies to asymptotically long times only, a comparison of simulation and theory concentrates on the exponential relaxation time

$$\tau_{\exp,\mathscr{A}} = \limsup_{t \to \infty} \frac{t}{-\ln|\Phi_{\mathscr{A}}(t)|} \tag{14}$$

Its scaling behavior with respect to lattice size L is described by the exponent z as

$$\tau_{\exp}(\varepsilon, L) = L^z \tau_{\exp,0}(L^{1/\nu}\varepsilon) \tag{15}$$

Here $\varepsilon = |T/T_c - 1|$ is the reduced temperature distance to the critical temperature.

In our Monte Carlo simulation, we analyze the three observables $\mathscr{M}$, $|\mathscr{M}|$, and $\mathscr{E}$. The purpose of studying several observables becomes evident from Eq. (13). It is reasonable to assume that all observables have a nonvanishing overlap $\rho_{\mathscr{A}}(\lambda^*)$ with the slowest mode (the contrary would assume exact orthogonality). But the one or other observable has significant measure $\rho_{\mathscr{A}}(\lambda)$ also for $\lambda < \lambda^*$, so that asymptotically one-exponential behavior is reached in different time ranges for different observables $\mathscr{A}$. In fact, it is the main difficulty of the analysis to identify this one-exponential region. According to the dynamic universality, it is expected that all observables have the same exponential relaxation time $\tau_{\exp,\mathscr{A}}$. This expectation has to be tested by simulations.

A different measure of the dynamical behavior inherent in the autocorrelation function (11) is the integrated relaxation time

$$\tau_{\text{int},\mathscr{A}} = \tfrac{1}{2} \sum_{t=-\infty}^{\infty} \Phi_{\mathscr{A}}(t) \tag{16}$$

which is a measure of *all* time scales that contribute to the relaxation of $\mathscr{A}$. Obviously, integrated relaxation times $\tau_{\text{int},\mathscr{A}}$ are smaller than exponential times $\tau_{\exp,\mathscr{A}}$. Moreover, $\tau_{\text{int},\mathscr{A}}$ is in general different for each observable $\mathscr{A}$. Surprisingly, there is no accurate numerical comparison of exponential and

integrated times so far for the three-dimensional Ising model. Since integrated relaxation times measure the decay of correlations in an integrated way, they are relevant for the calculation of the statistical errors of Monte Carlo estimates (9). The variance of a Monte Carlo estimate (9) based on n correlated values is[32, 33]

$$\mathrm{var}(\bar{\mathscr{A}}) = \frac{1}{n^2} \sum_{i,j}^{n} \phi_{\mathscr{A}}(i-j) \simeq \frac{1}{m} \phi_{\mathscr{A}}(0) \tag{17}$$

where

$$m = \frac{n}{2\tau_{\mathrm{int},\mathscr{A}}} \tag{18}$$

is the number of effectively uncorrelated $\mathscr{A}$-data of the time series. The determination of $\tau_{\mathrm{int},\mathscr{A}}$ is necessary in every Monte Carlo simulation to calculate the statistical errors of estimates.

Whereas dynamical finite-size scaling of $\tau_{\mathrm{exp},\mathscr{A}}$ in (15) is a result of the RG,[38, 39] there is no similar result for integrated relaxation times. In fact, there is no theoretical idea of whether the next-to-leading relaxation times $\tau < \tau_{\mathrm{exp}}$ scale and if they do, how their exponent z_τ differs from the asymptotic exponent z. In principle, one may conjecture the same power law behavior for integrated relaxation times

$$\tau_{\mathrm{int},\mathscr{A}} \equiv B_{\mathrm{int},\mathscr{A}} L^{z_{\mathrm{int},\mathscr{A}}} \tag{19}$$

with an exponent $z_{\mathrm{int},\mathscr{A}}$ valid for large enough L so that scaling corrections which affect $\tau_{\mathrm{exp},\mathscr{A}}$ as well as $\tau_{\mathrm{int},\mathscr{A}}$ are unmeasurably small. The exponent $z_{\mathrm{int},\mathscr{A}}$ depends on the scaling behavior of all time scales τ of (13) and on the generally *L-dependent* overlap of the observable with all modes of the dynamics. Apart from exceptional cases which allow for an exact solution of the dynamics,[33] we have no knowledge of $\tau_{\mathrm{int},\mathscr{A}}$ and its scaling behavior. Nevertheless, the determination of $\tau_{\mathrm{int},\mathscr{A}}$ for many observables $\mathscr{A}$ yields valuable information about the dynamics.

We complete our summary of notations with the power spectral density $P_{\mathscr{A}}(\omega)$. It is a favorable quantity to identify the long-time or low-frequency behavior of correlations. $P_{\mathscr{A}}(\omega)$ is the Fourier transform[36]

$$\begin{aligned} P_{\mathscr{A}}(\omega) &= \frac{1}{2\pi} \int_{-\infty}^{\infty} \phi_{\mathscr{A}}(t) \exp(-i\omega t)\, dt \\ &= \lim_{T \to \infty} \frac{1}{2T} \frac{1}{2\pi} \left[\int_{-T}^{T} \mathscr{A}(t) \exp(-i\omega t)\, dt \right]^2 \end{aligned} \tag{20}$$

of the autocorrelation function $\phi_{\mathscr{A}}(t)$. It contains exactly the same information as $\phi_{\mathscr{A}}(t)$, but the sampling properties of both quantities are very different, as we discuss in Section 3 and in the Appendix in connection with the Monte Carlo estimators of $\phi_{\mathscr{A}}(t)$ and $P_{\mathscr{A}}(\omega)$. Comparison with Eq. (16) shows that the integrated relaxation time is simply related to the normalized power spectral density

$$P_{0,\mathscr{A}}(\omega) \equiv \frac{P_{\mathscr{A}}(\omega)}{\phi_{\mathscr{A}}(\omega)} \tag{21}$$

by $P_{0,\mathscr{A}}(\omega = 0) = \tau_{\text{int},\mathscr{A}}/\pi$.

3. ESTIMATION OF AUTOCORRELATION FUNCTIONS AND POWER SPECTRAL DENSITIES

The estimation of thermodynamic quantities by averages over finite time series (9) has been well known from the beginning of Monte Carlo simulations. The calculation of their errors $\delta\bar{\mathscr{A}} = (\text{var}\,\bar{\mathscr{A}})^{1/2}$ necessitates the knowledge of time-dependent properties such as correlation functions (10) which are not easily estimated from a single time series. The estimation of time-dependent quantities has been solved in the theory of time series analysis.[36] Sokal and co-workers[33, 37] have summarized the essential results of this theory for application in Monte Carlo simulations. They have thoroughly discussed the estimation of correlation functions $\phi_{\mathscr{A}}(t)$, their variances, and the determination of the integrated relaxation times τ_{int}. We extend their discussion to the estimation of frequency-dependent quantities such as the power spectral density $P_{\mathscr{A}}(\omega)$ of (20). This estimation problem is treated in the second part of this section.

The estimation of correlation functions from a single time series relies on the assumption that the statistical properties of the process $\mathscr{A}(t)$ do not change over time. We assume that $\mathscr{A}(t)$ is stationary up to second order. Since we neglect fourth-order cumulants,[36] higher-order stationarity is not required. A *natural* estimator of the correlation function $\phi_{\mathscr{A}}(t)$ of (10) is given by the sum over the time series

$$\hat{\phi}_{\mathscr{A}}(t) \equiv \frac{1}{n - |t|} \sum_{s=t+1}^{n} (\mathscr{A}_s - \mu_{\mathscr{A}})(\mathscr{A}_{s-t} - \mu_{\mathscr{A}}) \tag{22}$$

where $\mu_{\mathscr{A}} \equiv \langle \mathscr{A} \rangle$ is the exact mean. In some cases, $\mu_{\mathscr{A}}$ is known from symmetry considerations, e.g., the mean $\mu_{\mathscr{M}}$ of the magnetization vanishes in the symmetric phase. If it is unknown, the estimator

$$\hat{\bar{\phi}}_{\mathscr{A}}(t) \equiv \frac{1}{n - |t|} \sum_{s=t+1}^{n} (\mathscr{A}_s - \bar{\mathscr{A}})(\mathscr{A}_{s-t} - \bar{\mathscr{A}}) \tag{23}$$

is appropriate, where $\bar{\mathscr{A}}$ is the estimated mean, Eq. (9). It has been shown in the theory of time series[36] that $\hat{\phi}_{\mathscr{A}}$ of (22) is an unbiased estimator of $\phi_{\mathscr{A}}$, whereas $\hat{\hat{\phi}}_{\mathscr{A}}$ of (23) is only asymptotically unbiased (i.e., in the limit $n \to \infty$). A typical example of our estimates $\hat{\hat{\Phi}}_{|\mathscr{M}|}$, $\hat{\hat{\Phi}}_{\mathscr{E}}$, and $\hat{\Phi}_{\mathscr{M}}$ is depicted in Fig. 1. For further discussion of modified estimators we refer to the standard literature.[36]

The bias of $\hat{\hat{\phi}}_{\mathscr{A}}$ in (23) in a finite time series with n steps results from the deviation of $\bar{\mathscr{A}}$ from $\mu_{\mathscr{A}}$. For large n it is given by

$$\phi_{\mathscr{A}}(t) = [\hat{\hat{\phi}}_{\mathscr{A}}(t)] + [(\bar{\mathscr{A}} - \mu_{\mathscr{A}})^2] = [\hat{\hat{\phi}}_{\mathscr{A}}(t)] + \frac{2\tau_{\text{int},\mathscr{A}}}{n} \phi_{\mathscr{A}}(0) \tag{24}$$

where the brackets $[\cdot]$ denote the average over the ensemble of n-step time series. Obviously, fluctuation estimators could be corrected for bias by (24) if necessary. However, the bias is an effect of order $1/n$, whereas the statistical errors to be discussed below are of the order $1/\sqrt{n}$, so that the bias can be neglected.

We shall mainly discuss the normalized correlation function $\Phi_{\mathscr{A}}(t)$ of (11), which is estimated by the ratio

$$\hat{\Phi}_{\mathscr{A}}(t) \equiv \frac{\hat{\phi}_{\mathscr{A}}(t)}{\hat{\phi}_{\mathscr{A}}(0)} \tag{25}$$

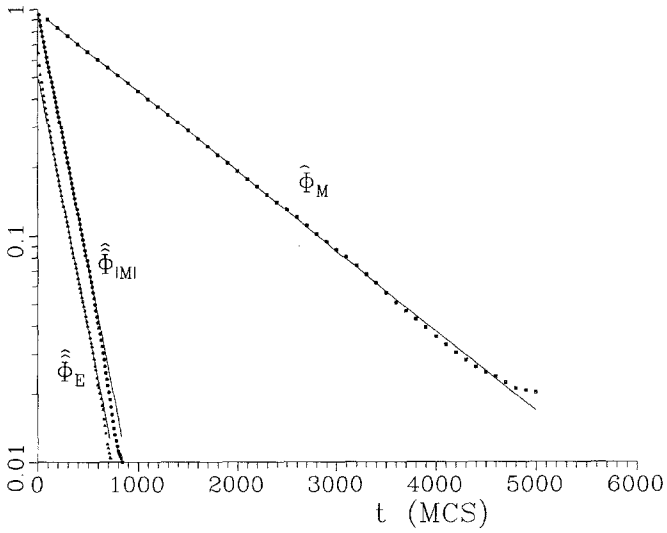

Fig. 1. Correlation function estimates $\hat{\Phi}_{\mathscr{M}}$, $\hat{\hat{\Phi}}_{|\mathscr{M}|}$, and $\hat{\hat{\Phi}}_{\mathscr{E}}$ of 50^3 lattices calculated from 19×10^6 lattice updates. The straight lines are one-exponential fits in the asymptotic range (see Table III).

of estimators $\hat{\phi}_{\mathscr{A}}(t)$ and $\hat{\hat{\phi}}_{\mathscr{A}}(t)$, respectively. The sampling properties of the sample autocorrelation function $\hat{\Phi}_{\mathscr{A}}(t)$ are more complicated because $\hat{\Phi}_{\mathscr{A}}$ is a ratio of correlated random variables. It is a fundamental result due to Bartlett[40] that the covariance of $\hat{\Phi}_{\mathscr{A}}(t)$ is given by

$$\begin{aligned}
&\operatorname{cov}(\hat{\Phi}_{\mathscr{A}}(t), \hat{\Phi}_{\mathscr{A}}(t+t')) \\
&\simeq \frac{1}{n} \sum_{s=-\infty}^{\infty} \{\Phi_{\mathscr{A}}(s)\, \Phi_{\mathscr{A}}(s+t) \\
&\quad + \Phi_{\mathscr{A}}(s+t+t')\, \Phi_{\mathscr{A}}(s-t) + 2\Phi_{\mathscr{A}}(t)\, \Phi_{\mathscr{A}}(t+t')\, \Phi_{\mathscr{A}}^2(s) \\
&\quad - 2\Phi_{\mathscr{A}}(t)\, \Phi_{\mathscr{A}}(s)\, \Phi_{\mathscr{A}}^2(s-t-t') - 2\Phi_{\mathscr{A}}(t+t')\, \Phi_{\mathscr{A}}(s)\, \Phi_{\mathscr{A}}^2(s-t)\}
\end{aligned} \tag{26}$$

neglecting the fourth-order cumulants.[36] Since we are interested in correlation functions of asymptotically exponential type, we conveniently assume $\Phi_{\mathscr{A}}(t) \simeq \exp(-t/\tau_{\mathscr{A}})$ and $\tau_{\mathscr{A}} \gg 1$. This ignores the next-to-leading time scales,[37] an assumption which is reasonable in view of the long-time behavior of correlation functions (Fig. 1). For $t, t+t' > 0$, we then obtain from Eq. (26)

$$\begin{aligned}
&\operatorname{cov}(\hat{\Phi}_{\mathscr{A}}(t), \hat{\Phi}_{\mathscr{A}}(t+t')) \\
&\simeq \frac{\tau_{\mathscr{A}}}{n} e^{(-|t'|/\tau_{\mathscr{A}})} \left[1 + \frac{|t'|}{\tau_{\mathscr{A}}} - e^{(-2t/\tau_{\mathscr{A}})} \left(1 + \frac{2t+t'}{\tau_{\mathscr{A}}}\right)\right]
\end{aligned} \tag{27}$$

This result shows that the variance and covariance of $\hat{\Phi}_{\mathscr{A}}$, respectively, depend on the relaxation time $\tau_{\mathscr{A}}$ in the same way as the variance of ordinary static properties, such as mean values $\overline{\mathscr{A}}$ and fluctuations $\overline{\mathscr{A}^2}$. It is the same number $m = n/2\tau_{\mathscr{A}}$, Eq. (18), of effectively uncorrelated measurements that determines the errors of all estimators. To be precise, the variance $\operatorname{var}(\hat{\Phi}_{\mathscr{A}}(t))$ in (27) increases from $\operatorname{var}(\hat{\Phi}_{\mathscr{A}}(0)) = 0$ to $\tau_{\mathscr{A}}/n$ for long times. Because of the normalization $\hat{\Phi}_{\mathscr{A}}(t=0) = 1$ of the estimates, this behavior differs from that of the variance $\operatorname{var}(\hat{\phi}(t)) = \operatorname{cov}(\hat{\phi}(t), \hat{\phi}(t))$ of the unnormalized correlation function $\phi_{\mathscr{A}}(t)$ given by Beretti and Sokal.[37]

The covariance is dominated by the leading exponential term in (27). It shows that $\operatorname{cov}(\hat{\Phi}_{\mathscr{A}}(t), \hat{\Phi}_{\mathscr{A}}(t+t'))$ decreases with the same time scale $\tau_{\mathscr{A}}$ as the correlation function itself. Consequently, there is a fairly high correlation between neighboring points of the series $\{\hat{\Phi}_{\mathscr{A}}(t)\}$ leading to smooth sequences of correlation data. The ratio

$$\frac{\operatorname{cov}(\hat{\Phi}_{\mathscr{A}}(t), \hat{\Phi}_{\mathscr{A}}(t+t'))}{\operatorname{var}(\hat{\Phi}_{\mathscr{A}}(t))} \simeq \exp\left(\frac{-|t'|}{\tau_{\mathscr{A}}}\right) \tag{28}$$

is a measure of the smoothness of the data sequence. It is independent of the precision of the data. Thus, statistically good and bad data cannot be distinguished from the visual impression of the data. It is indispensable to calculate their variances explicitly. One should be aware of the high covariance when one tries to identify systematic deviations of measured correlation data from their expected time dependence. The high covariance may lead to misinterpretations in this case.

We have compared the calculated error $\delta\hat{\Phi}_{\mathscr{A}} = (\text{var}\,\hat{\Phi}_{\mathscr{A}})^{1/2}$ following from (27) with the measured errors. The latter have been estimated from an ensemble of records each with a fixed number of time steps. The errors in Table II refer to the point $\Phi_{\mathscr{A}} \simeq 0.1$ and have been calculated for $\mathscr{M}$ and $|\mathscr{M}|$. The agreement is satisfactory and indicates that the assumptions leading to (27) are roughly fulfilled. The comparison of the errors of $\hat{\Phi}_{|\mathscr{M}|}$ and of $\hat{\Phi}_{\mathscr{M}}$ show that the former is a factor 2.5 smaller. According to (27), this follows from the ratio $\tau_{\mathscr{M}}/\tau_{|\mathscr{M}|} \simeq 6$, which is a result of our simulation (see Section 6). The dependences of the relative error $\delta\hat{\Phi}_{|\mathscr{M}|}/\hat{\Phi}_{|\mathscr{M}|}$ on time and Φ, respectively, are depicted in Fig. 2. They are well described by our result (27).

The estimation of the power spectral density $P_{\mathscr{A}}(\omega)$ of (20) is less straightforward. It appears natural to estimate $P_{\mathscr{A}}(\omega)$ by its sample version as

$$I_n(\omega) = 2\left\{\hat{\phi}(0) + 2\sum_{t=1}^{n-1}\hat{\phi}(t)\cos\omega t\right\}$$
$$= \frac{2}{n}\left\{\left|\sum_{t=1}^{n}\mathscr{A}(t)\cos\omega t\right|^2 + \left|\sum_{t=1}^{n}\mathscr{A}(t)\sin\omega t\right|^2\right\} \tag{29}$$

Table II. Comparison of Estimated and Calculated Errors of Our Final Correlation Function Estimates $\hat{\Phi}_{|\mathscr{M}|}$ and $\hat{\Phi}_{\mathscr{M}}$ after Averaging over All Data[a]

L	$\delta\hat{\Phi}_{\lvert\mathscr{M}\rvert}$ $(\Phi \approx 0.1)$	$\delta\hat{\Phi}_{\lvert\mathscr{M}\rvert,C}$	$\delta\hat{\Phi}_{\mathscr{M}}$ $(\Phi \approx 0.1)$	$\delta\hat{\Phi}_{\mathscr{M},C}$
20	1.4×10^{-3}	2.1×10^{-3}	3.0×10^{-3}	5.4×10^{-3}
26	1.9×10^{-3}	1.9×10^{-3}	7.2×10^{-3}	4.9×10^{-3}
30	2.5×10^{-3}	2.0×10^{-3}	9.4×10^{-3}	5.2×10^{-3}
36	2.1×10^{-3}	2.1×10^{-3}	4.6×10^{-3}	5.3×10^{-3}
40	1.6×10^{-3}	2.2×10^{-3}	4.3×10^{-3}	5.7×10^{-3}
46	2.0×10^{-3}	2.8×10^{-3}	7.1×10^{-3}	6.8×10^{-3}
50	1.7×10^{-3}	3.2×10^{-3}	5.2×10^{-3}	8.1×10^{-3}
60	3.7×10^{-3}	3.6×10^{-3}	7.2×10^{-3}	8.9×10^{-3}

[a] The values correspond to correlation function estimates $\Phi \approx 0.1$. There is a fairly good agreement between estimated (columns 2 and 4) and calculated (columns 3 and 5) errors. The ensembles (Table I) are small, so that the error estimates are very rough.

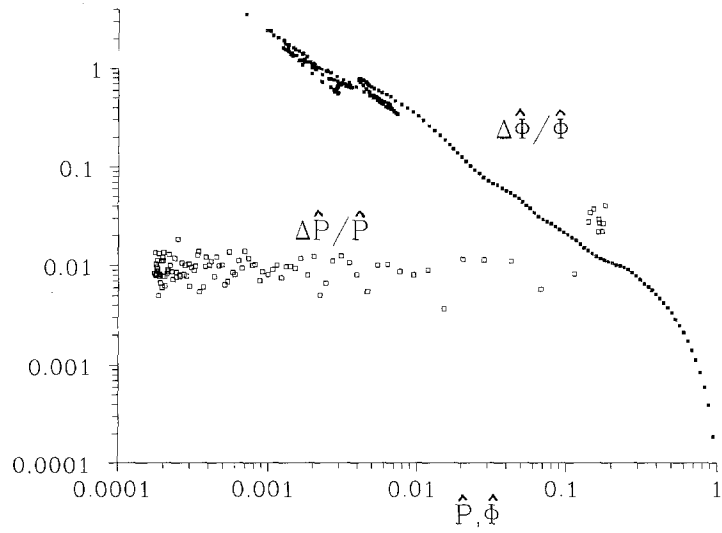

Fig. 2. Relative errors of estimates of the correlation function $\hat{\Phi}_{|\mathscr{M}|}$ and of the power spectral density $\hat{P}_{|\mathscr{M}|}$ determined from single simulations of 46^3 lattices (Table I). The errors are in good accord with Eqs. (27) and (A13), respectively. Similar error dependences have been obtained for all lattices. Notice that large values of P correspond to small frequencies ω. In this limit we have chosen a large window parameter $n_0 \simeq 1000$ for a better resolution of the smooth crossover to the finite-size limit described by Eq. (44). The mean square errors are larger then, as described by Eq. (A13).

which is called the periodogram.[36] Comparison with (20) shows that $I_n(\omega)$ has to be a multiplied by a factor $1/4\pi$ to be an estimator of $P(\omega)$. The function

$$\hat{I}^*(\omega) = \frac{1}{4\pi} I_n(\omega) \tag{30}$$

is called the sample spectral density function. It is defined on the standard grid

$$\omega = \omega_p = \frac{2\pi p}{n} \qquad \left(p = 0, 1, ..., \frac{n}{2}\right) \tag{31}$$

The sampling properties of $I^*(\omega)$ are extremely bad: It is an unbiased, but not a consistent estimator of the power spectral density $P(\omega)$.[36] This means that it does not converge to $P(\omega)$ in mean square. In fact, its variance $\mathrm{var}(\hat{I}_n^*(\omega))$ is of $O(1)$ even for $n \to \infty$ and the covariance $\mathrm{cov}(\hat{I}_n^*(\omega_1), \hat{I}_n^*(\omega_2))$ decreases for $n \to \infty$, leading to a wildly fluctuating $\hat{I}_n^*(\omega)$. The bad statistical behavior of the periodogram is an instructive

example that a natural estimator may be statistically useless. This phenomenon has been studied in the theory of time series analysis,[36] and other estimators for $P(\omega)$ which are consistent and asymptotically unbiased have been provided. The problem has been discussed by Madras and Sokal[33] and by Wolff[41] in conjunction with the estimation of integrated relaxation times $\tau_{\text{int},\mathscr{A}}$:

In our work we make use of the Daniell or rectangular window [Appendix, Eq. (A10)] to obtain a smoothed estimator (see Appendix). This choice is motivated by practical reasons: we simulate 64 lattices with different relaxation times in a single run each with several million data for each observable. This necessitates a fast and easy implementation. The Daniell window parameter n_0 of Eq. (A10) is chosen near its optimum value (A15) to minimize the total error of the estimate $\hat{P}_n(\omega)$ of Eq. (A3). The optimum value of n_0 depends on n and on the normalized curvature $P''(\omega)/P(\omega)$. Instead of calculating optimal values $n_0(\omega)$ for each frequency, we conveniently choose a larger than optimal value in the low-frequency limit $\omega < O(1/2\tau)$ to obtain a better frequency resolution and a smaller value in the high-frequency limit $[\omega > O(1/2\tau)]$. We point out that our final data are averaged over small ensembles of independent runs of record length n_{upd} (Table I) each of which is analyzed separately. Finally, we perform an average of $\hat{P}_n(\omega)$ [as well as $\hat{\Phi}(t)$] over all runs. This procedure, which is demanded by the maximum vector length on our computer, is less optimal than the analysis of an equivalent single run, since the bias, Eq. (A6), is slightly larger in this case. To compensate for that, it is advisable to choose the window parameter n_0 according to the total record length of all runs. These considerations show that part of a proper data analysis has to be done in the planning phase of a simulation to make the most of the available data.

As an example of our analysis, Fig. 2 compares the relative errors of the estimates $\hat{P}_{|\mathscr{M}|}(\omega)$ of the power spectral density to those of the correlation function $\hat{\Phi}_{|\mathscr{M}|}(t)$. Both data sets are calculated from the same time series. It is obvious that the estimation of the power spectral density is better by two orders of magnitude compared to the correlation function in the interesting long-time (low-frequency) limit. Typical relative errors of the estimator $\hat{P}(\omega)$ of Eq. (A3) are in the range

$$\frac{\delta \hat{P}_n(\omega)}{\hat{P}_n(\omega)} \simeq 5 \times 10^{-3}\text{–}10^{-2} \tag{32}$$

depending on the total amount of data. Comparison with the relative error of $\hat{\Phi}_{\mathscr{A}}(t)$, Eq. (27), shows that the power spectral density $P(\omega)$ is well suited to investigate the long-time behavior of Monte Carlo time series.

It will be useful in order to identify the asymptotic time range of one-exponential decay. This is necessary for a proper determination of exponential relaxation times.

4. SCALING PROPERTIES OF THE CORRELATION FUNCTION AND THE POWER SPECTRAL DENSITY

The time and frequency dependences of $\Phi_{\mathscr{A}}(t)$ and $P_{\mathscr{A}}(\omega)$, respectively, are largely unknown. Knowledge of them is equivalent to complete information about the spectrum (13) of the Liouville operator in the limit of infinite state space $\mathscr{Q}$. In fact, the RG approaches[38, 39] extract the dynamical exponent z from the scaling of the largest time scale, but they do not yield any information about next-to-leading time scales and their scaling behavior.

In Monte Carlo simulations we are concerned with a finite system. The largest eigenvalue λ^* (Section 2) yields the (finite) exponential relaxation time $\tau_{\exp,\mathscr{A}}$, which is the largest time scale of the system unless the observable $\mathscr{A}$ is accidentally orthogonal to the slowest mode. The Monte Carlo analysis which aims at the calculation of z in (15) is confronted with the severe problem to extract the exponential time scale from correlation function estimates without much information about the true time dependence of $\Phi(t)$. We know that there is a largest (exponential) relaxation time, but we do not know the exponential time region where this time scale dominates. Strictly speaking, the problem is ill posed as long as we do not know an upper bound of the exponential relaxation time of the finite system.

The extraction of $\tau_{\exp,\mathscr{A}}$ from equilibrium correlation data has been done in a rather pragmatic way in the past. The large-scale simulation by Pearson *et al.*[16] was analyzed by applying the definition of $\tau_{\exp,\mathscr{A}}$ in (14) in a direct way. The authors simply *observed* a leveling off of the local derivatives of $\hat{\Phi}_{\mathscr{A}}(t)$. It is clear that this method suffers from the same concurrence of bias (due to estimate of the derivative at finite time) and variance (due to increasing variance with time) as the determination of the integrated relaxation time.[33, 41] Pearson *et al.*[16] did not give a quantitative criterion for the exponential time region they assumed for their final estimate of $\tau_{\exp,\mathscr{A}}$. A recent simulation by Wansleben and Landau[20] was analyzed in a completely different way. In order to utilize the correlation data for all times—being aware that the smaller times have smaller errors—the authors fitted their correlation data to a two- and three-exponential ansatz. But it is by no means clear that the replacement of a large number of exponentials ($2^{125000} \simeq 10^{38000}$ for a 50^3 system) by two or three exponentials should yield a sensible description. Instead it is well

known that in the short-time region the exponentials add up to an algebraic decay of correlations[42] as in the infinite system.

It appears reasonable to summarize some facts about correlation functions and power spectral densities in the critical region which are easily verified by our data. The dynamic scaling hypothesis[2] of the low-frequency behavior of the power spectral density $P_{\mathscr{A}}(\omega)$ of (20) is readily extended to finite systems by[42]

$$P_{\mathscr{A}}(\omega, L) = b^{2-\eta+z-d} P_{\mathscr{A}}(b^z\omega, b^{-1}L) = L^{2-\eta+z-d} P_{\mathscr{A},0}(\omega L^z) \quad (33)$$

Notice that the scaling of $P_{\mathscr{A}}$ contains an additional factor b^{-d}. This is due to the fact that fluctuations of densities like $\phi_{\mathscr{A}}(t)$ and their Fourier transform $P_{\mathscr{A}}(\omega)$ have to be multiplied by the volume L^d to obtain the usual scaling in the thermodynamic limit. Figure 3 shows an example of the scaling of $\hat{P}_{|\mathscr{M}|}(\omega, L)$ resulting from our simulation.

By Fourier transformation (20), Eq. (33) is equivalent to the scaling form

$$\phi_{\mathscr{A}}(t, L) = b^{2-\eta-d} \phi_{\mathscr{A}}(b^{-z}t, b^{-1}L) = L^{2-\eta-d} \phi_{\mathscr{A},0}(tL^{-z}) \quad (34)$$

of the correlation function $\phi_{\mathscr{A}}(t)$, Eq. (10). Both scaling forms have been shown to be valid in the long-time or low-frequency limit by the dynamic RG.[2] However, the onset of scaling with respect to time t or frequency ω

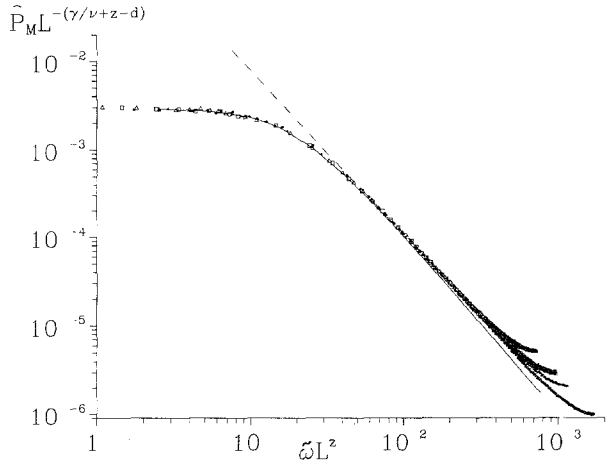

Fig. 3. Estimates $\hat{P}(\omega)$ of the power spectral density plotted in scaling form using the theoretical value $\gamma/\nu = 1.97$ and our result $z = 2.09$ for the dynamic exponent. In the asymptotic range, the form is Lorentzian, Eq. (44) (solid curve); for large frequencies, we find bulk behavior described by Eq. (35) (dashed curve).

is as unknown as the critical region itself and the scaling region of system size L. The RG does not provide information about these nonuniversal features of the dynamics.

It has been pointed out by Angles d'Auriac *et al.*[42] that the power spectral density (20) diverges algebraically,

$$L^d P_{\mathscr{A}}(\omega, L) \sim \omega^{-\mu_{\mathscr{A}}} \tag{35}$$

with the exponents

$$\begin{aligned} \mu_{\mathscr{M}} &= 1 + \frac{\gamma}{\nu z} \\ \mu_{\mathscr{E}} &= 1 + \frac{\alpha}{\nu z} \end{aligned} \tag{36}$$

in the large-frequency limit $\omega \geqslant \tau_{\exp}^{-1}$ (bulk range of the finite system). In this frequency range, the finite system behaves like the infinite system. The power-law behavior (35) is characteristic for self-similar processes, as Kolmogorov showed very early.[43] In the bulk range, the processes $\mathscr{M}(t)$ and $\mathscr{E}(t)$ are fractal Brownian processes with a fractal dimension $D = (5 - \mu)/2$. We have verified this behavior in Fig. 4 by means of the structure function $\Psi(t) = |\mathscr{A}(t' + t) - \mathscr{A}(t')|^2$, which obeys the power law

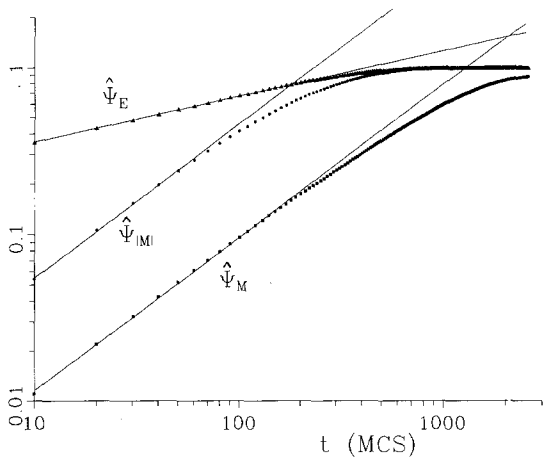

Fig. 4. The structure function $\Psi(t)$ defined in Section 4, showing power law behavior for short times. We find $\mu_{\mathscr{M}} \simeq \mu_{|\mathscr{M}|} \simeq 1.92$, in good accord with the expected value 1.94 using our result $z = 2.09$. For the energy structure function $\Psi_{\mathscr{E}}(t)$ we fit the data with an exponent $\mu_{\mathscr{E}} = 1.28$, which is much larger than the expected value 1.08. This discrepancy originates from short relaxation times which scale in a different way than the exponential time $\tau_{\exp,\mathscr{E}}$.

$\Psi(t) \sim t^{\mu_{\mathscr{A}}-1}$ in the bulk range.[43] However, the time window for bulk behavior (35) is too small to fit $\mu_{\mathscr{A}}$ and z, respectively, to high accuracy (Fig. 4). The crossover from the bulk from (35) to the finite-size asymptotic (39) and (38) to be discussed below leads to considerable curvature, so that the value of z depends on the time interval of the fit (Fig. 4). By the relation $\Psi_{\mathscr{A}}(t) = 2[\Phi_{\mathscr{A}}(0) - \Phi_{\mathscr{A}}(t)]$, it is shown that the normalized correlation function $\Phi_{\mathscr{A}}(t)$ of (11) has an algebraic time dependence,[43]

$$\Phi_{\mathscr{A}}(t) = 1 - cL^{-\gamma/\nu} t^{\mu_{\mathscr{A}}-1} \tag{37}$$

in the bulk region $t \leqslant \tau_{\exp}$. It is equivalent to the power law behavior of $\Psi(t)$ verified above.

We now turn to the asymptotic time range of finite systems and propose a method to determine $\tau_{\exp}$ in a systematic way (we leave out the subscript $\mathscr{A}$ for the observable to lighten the notation henceforth). As we have discussed in Section 3, the estimator of the power spectral density is much better suited to analyzing the long-time behavior of a process than the estimator of the correlation function. However, there is a slight disadvantage in using $P(\omega)$ in the region of small ω. This is due to the fact that the power spectral density $P(\omega)$ is an integral over the whole spectrum $\rho(\tau)$ of relaxation times, which has maximum weight at $\tau_{\exp}$ and a tail toward smaller relaxation times.

In order to discuss the frequency dependence of $P(\omega)$ we assume for the moment a simple one-exponential behavior

$$\phi_{\mathscr{A}}(t, L) = C \exp(-t/\tau_{\exp}) \qquad \text{with} \quad \tau_{\exp} = AL^z \tag{38}$$

valid for all times. The amplitude scales as $C \sim L^{2-\eta-d}$ according to Eq. (34). The power spectral density $P_{\mathscr{A}}(\omega)$ of (20) corresponding to a one-exponential $\phi(t)$, Eq. (38), has the Lorentzian form and scales as

$$P(\omega, L) = \frac{C}{\pi} \frac{\tau_{\exp}}{1 + \omega^2 \tau_{\exp}^2} = L^{2-\eta+z-d} \frac{1}{\pi} \frac{A}{1 + A^2(\omega L^z)^2} \tag{39}$$

It is obvious from Fig. 3 that $P_{|\mathscr{M}|}(\omega, L)$ deviates from the Lorentzian form (39) for large frequencies (bulk range) as discussed above.

The tail of the spectrum, which we have ignored in (38) and (39), leads to a modification of the simple Lorentzian form (39). With Eqs. (13) and (20), one obtains an expansion of the normalized power spectral density $P_0(\omega)$ of (21) in terms of moments of the spectrum $\tilde{\rho}$:

$$P_0(\omega) = \frac{1}{\pi} \int \tilde{\rho}(\tau') \frac{\tau_{\exp} + \tau'}{1 + \omega^2(\tau_{\exp} + \tau')^2} \, d\tau' \tag{40}$$

Here, $\tilde{\rho}(\tau') = \rho(\tau_{\exp} + \tau')$ is nonzero only for $\tau' < 0$. We expand $P_0(\omega)$ in (40) in powers of ω^2:

$$P_0(\omega) = P_0^{(0)} + P_0^{(2)}\omega^2 + O(\omega^4) \tag{41}$$

The first term is the integrated relaxation time $\tau_{\text{int}}/\pi = P_0^{(0)}$, Eq. (16). Thus, the first moment of the distribution $\tilde{\rho}$ of relaxation times is the difference of integrated and exponential relaxation times:

$$\int \tilde{\rho}(\tau')\tau' \, d\tau' = \tau_{\text{int}} - \tau_{\exp} \tag{42}$$

The second-order term is given by

$$P_0^{(2)} \simeq -\frac{1}{\pi}\tau_{\exp}^3 \left(1 + 3\,\frac{\tau_{\text{int}} - \tau_{\exp}}{\tau_{\exp}}\right) \tag{43}$$

neglecting the second and higher moments of $\tilde{\rho}$ compared to the first moment. This is motivated by the expectation that the tail of the spectrum drops rather sharply, so that the relative difference of τ_{int} and $\tau_{\exp}$ contains the leading correction of the simple one-exponential behavior. This assumption imposes a restriction to the applicability of our method: processes with broad or complicated spectra will not be treated adequately in this simplified way, which neglects higher moments of the spectrum $\tilde{\rho}$. Improving the method would necessitate the calculation of higher moments of $\tilde{\rho}$ from the data.

Introducing the ratio $C = L^{2-\eta-d}\tau_{\text{int}}/\tau_{\exp}$, we can write Eq. (41) similar to the simple Lorentz form (39), taking into account the leading corrections of nonexponential time scales:

$$P(\omega) = \frac{C}{\pi}\frac{\tau_{\exp}}{1 + \omega^2\tau_{\exp}^2 k(C)} + O(\omega^4) \tag{44}$$

with $k(C) = [1 + 3(C-1)]/C$. This approximation of the low-frequency behavior of the power spectral density is the starting point of our analysis: we first calculate the integrated relaxation time τ_{int} from our estimates of the correlation function. This will be done in Section 6 by well-known methods.[33, 41] Then we estimate the exponential relaxation time $\tau_{\exp}$ by fitting our correlation function estimates to a simple exponential decay in a preliminary long time interval where we hope to be in the asymptotic limit (being aware that we cannot prove it). With these values of $\tau_{\exp}$ and τ_{int} we calculate the power spectral density $P(\omega)$ in the approximation (44). Since our values of $\hat{P}(\omega)$ are much more accurate than those of $\hat{\Phi}(t)$, we

can neatly observe the onset of deviations of our measured $\hat{P}$ data from the calculated curve (see Fig. 3). The frequency ω_c and time $t_c = 2\pi/\omega_c$, respectively, where the deviation exceeds the error of $\hat{P}(\omega)$ are the limits of the asymptotic time range. In this asymptotic time range we fit our correlation data to a simple exponential and arrive at our final estimates for τ_{exp}.

5. ODD AND EVEN OBSERVABLES

Before we present the quantitative results obtained by this method, we discuss the different dynamical behavior of odd and even observables. We pointed out in Section 2 that it is reasonable to study several observables because of their different overlap with the slowest mode of the system. The symmetry of an observable is of great importance in this respect. The Ising model at zero magnetic field is invariant under global spin flips and the dynamics commutes with this global spin flip. Thus, the eigenvectors of the Liouville operator are also eigenvectors of the inversion operator with eigenvalues ± 1. The dynamical time evolution of odd and even observables is separated into an odd and an even subspace, respectively.

The static critical behavior is dominated by a single length scale ξ, the correlation length, if hyperscaling is valid. The divergence of magnetic and energetic properties is described by this length scale. Dynamic critical phenomena are expected to be similarly characterized by a single time scale τ_{exp}, independent of the observable under consideration. This is expected in the asymptotic limit of large system sizes and long times.

In finite lattices no true symmetry breaking can occur. The dynamical consequence is a *lack* of ergodicity breaking. This is an annoying feature in Monte Carlo simulations, where one observes the system jumping from positive to negative values of $\mathcal{M}$, Eq. (4), in the ordered phase $T < T_c$ of the infinite system. This behavior has already been described.[44] Here, we emphasize the fact that this behavior of finite lattices persists *at* the critical temperature T_c of the infinite system where finite-size simulations are performed.

It is necessary to distinguish three different regimes (Fig. 5): (I) the high-temperature, infinite-volume limit ($L \to \infty$) at fixed $T > T_c$; (II) the low-temperature, infinite-volume limit at fixed $T < T_c$; (III) the finite-size scaling regime, which has a bulk ($\xi \ll L$) and a finite-size ($\xi \gg L$) limit. In the scaling regime III the exponential relaxation time is described by $\tau(\xi, L) = \xi^z f(\xi/L)$ or equivalently by $\tau = L^z g(\xi/L)$.

The sign fluctuations of odd observables in finite lattices lead to very different relaxation times of odd and even observables in the low-temperature regime II and in the interval $T < T_c$ of the scaling regime III. While $\tau_{\text{exp, even}} = O(1)$ in II, the relaxation time $\tau_{\text{exp, odd}}$ of odd observables increases

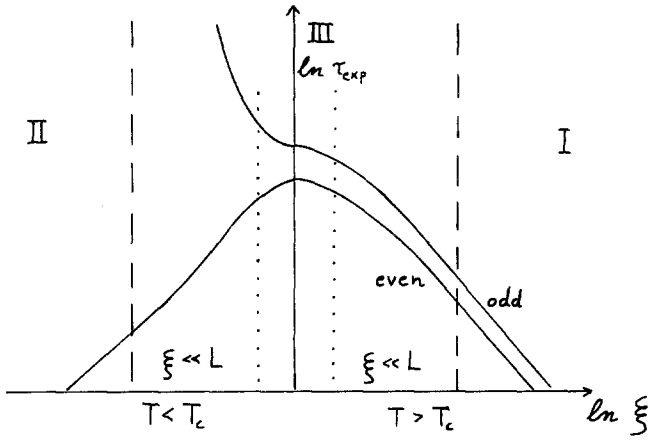

Fig. 5. Schematic plot of the exponential relaxation times τ_{exp} of odd and even observables of a *finite* system. The dashed lines roughly separate the regions I and II from the scaling region III. The dotted lines separate the bulk range of simulations $\xi \ll L$ from the finite-size range $\xi \gg L$.

exponentially with lattice size L as $\tau_{exp,\,odd} \sim \exp[\sigma(T) L^{d-1}]$.[39, 45] It is strictly infinite in the thermodynamic limit $L \to \infty$ for all $T \leqslant T_c$. The origin of this behavior is the creation of domain walls in finite systems whose activated movement leads to sign changes. At low temperatures in regime II, these sign flips do not occur within reasonable Monte Carlo simulation times; one observes fluctuations with short correlations in one phase only. With increasing temperature but still $T < T_c$, one enters a subtle region (Fig. 6a): the event of sign flip occurs more frequently and the time average (9) of odd observables $\mathscr{A}$ drops from $\bar{\mathscr{A}} \simeq A$ to $\bar{\mathscr{A}} \simeq 0$ although the *infinite* system is still deeply in the ordered phase. Consequently, the dynamical behavior which is measured by the estimator $\hat{\phi}$ of (23) for low temperatures has to be estimated by $\hat{\phi}$ of (22). Figure 6 shows that processes $\mathscr{A}(t)$ of odd observables possess two time scales which describe different phenomena: the longer time scale originates from fluctuations of the sign of $\mathscr{A}$, the shorter from fluctuations of the absolute value $|\mathscr{A}|$. This feature extends up to temperatures slightly above T_c.

We have analyzed this mixed process at the critical temperature T_c of the infinite system by splitting the odd observable $\mathscr{M}(t)$ into its sign, $\text{sign}(\mathscr{M})(t)$, and its absolute value $|\mathscr{M}|\,(t)$. The appropriate correlation function estimators $\hat{\phi}_{\mathscr{M}}(t)$, $\hat{\phi}_{\text{sign}(\mathscr{M})}(t)$, and $\hat{\phi}_{|\mathscr{M}|}(t)$ in Fig. 7 confirm the qualitative impression of Fig. 6: Comparising $\hat{\phi}_{\text{sign}(\mathscr{M})}$ with $\hat{\phi}_{\mathscr{M}}(t)$ shows clearly that the dominant contribution to the dynamical behavior of odd observables is the fluctuation of the sign. We find that in the three-dimensional Ising model the exponential relaxation time $\tau_{exp,\,odd}$ of odd

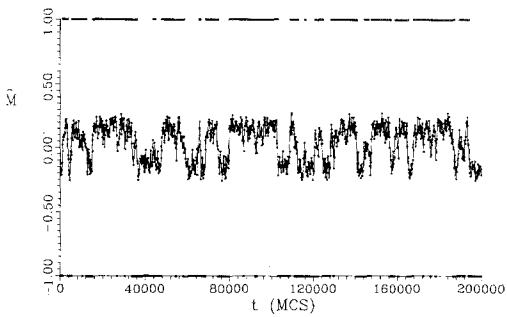

(a)

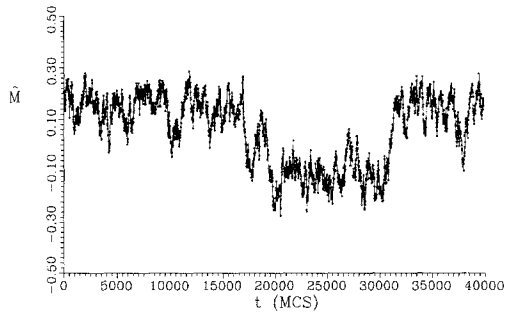

(b)

Fig. 6. (a) A record of the observable $\mathcal{M}(t)$ of a 60^3 system at the critical temperature $T_c = 4.51154$ of the infinite system. Fluctuations of the sign of $\mathcal{M}$ dominate the long-time behavior of $\hat{\Phi}_{\mathcal{M}}$ (Fig. 7). (b) Part of the $\mathcal{M}(t)$ record with a higher resolution. It is evident that fluctuations of $\mathcal{M}(t)$ are composed of fluctuations of the sign and the magnitude with distinctly different time scales.

observables is about a factor six larger than $\tau_{\text{exp, even}}$ at the critical temperature. This nontrivial ratio

$$\tau_{\text{odd}}/\tau_{\text{even}} = f(L/\xi) \tag{45}$$

depends on the double-welled free energy functional of finite lattices at T_c. It is expected that $f(L/\xi)$ is a universal scaling function in the finite-size scaling regime III, depending only on the universality class of the system. Universality is not expected in the low-temperature regime I and that part of the scaling regime III where the exponential L dependence crosses over to the power-law behavior $\tau_{\text{odd}} \sim L^z$. We have also performed simulations in the bulk limit of the scaling regime III above T_c and we find that the scaling function $f(L/\xi)$ of (45) smoothly approaches $f(\infty) \simeq 2$.

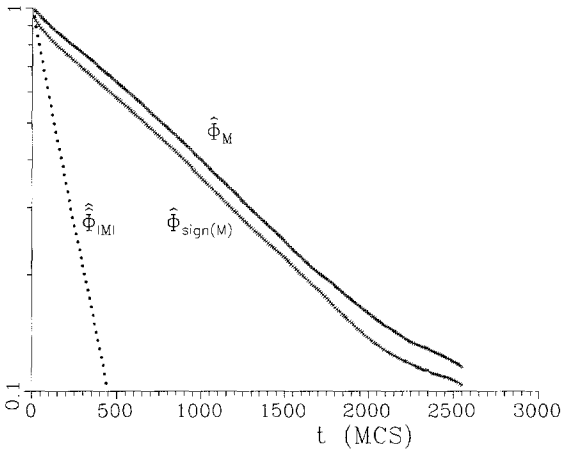

Fig. 7. Correlation function estimates of $\Phi_{\mathcal{M}}$, $\Phi_{|\mathcal{M}|}$, and $\Phi_{\mathrm{sign}(\mathcal{M})}$. The exponential time scales $\tau_{\exp,\mathcal{M}}$ and $\tau_{\exp,\mathrm{sign}(\mathcal{M})}$ are identical. The exponential relaxation time of even observables like $|\mathcal{M}|$ is about a factor six shorter.

6. INTEGRATED AND EXPONENTIAL RELAXATION TIMES

The estimation of integrated relaxation times from correlation function estimates is performed in the way discussed by Madras and Sokal[33] and Wolff.[41] Both schemes cut off the time integral and sum [Eq. (16)], respectively, at some window parameter n_0:

$$\hat{\tau}_{\mathrm{int}} = \tfrac{1}{2} + \sum_{t=1}^{n_0-1} \hat{\Phi}(t)\,\lambda(t) + R(n_0) \tag{46}$$

Madras and Sokal[33] omit the residual term $R(n_0)$, which leads to a bias

$$b(\hat{\tau}_{\mathrm{int}}) = \sum_{t \geqslant n_0} \Phi(t) \tag{47}$$

In his scheme, Wolff[41] extrapolates the integrated relaxation time using the local derivative of $\hat{\Phi}(n_0)$ for extrapolation:

$$R(n_0) = \hat{\Phi}(n_0)\left[1 - \frac{\hat{\Phi}(n_0)}{\hat{\Phi}(n_0-1)}\right]^{-1} \tag{48}$$

Both methods yield a consistent estimate for τ_{int} in the limit $n_0/n \to 0$ and $n \to \infty$.

The method of Madras and Sokal has a considerable bias. This necessitates a large window parameter n_0. Madras and Sokal[33] suggest a

self-consistent cutoff parameter $n_0 \geqslant c\tau_{\text{int}}$. The value of c depends on the process under discussion: Minimizing the mean square error $\eta^2 = \text{var} + b^2$, which consists of the variance[33] $\text{var} = 4\tau_{\text{int}}^2 n_0/n$ and the bias b, eq. (47) leads to

$$\frac{n_0}{\tau_{\text{int}}} \simeq \frac{1}{2} \ln \frac{n}{2\tau_{\text{int}}} - \ln[\tau_{\text{int}}(1 - e^{(-1/\tau_{\text{int}})}] \tag{49}$$

The optimal value of n_0/τ_{int} depends essentially on the number of effectively uncorrelated data $n/2\tau_{\text{int}}$; the second term in Eq. (49) is negligible. For typical simulations with $n/2\tau_{\text{int}} = O(10^4\text{–}10^5)$ Monte Carlo steps one obtains $c \simeq 5\text{–}6$. The estimation of $\tau_{\text{int},\mathscr{A}}$ for our three observables $\mathscr{M}$, $|\mathscr{M}|$, and $\mathscr{E}$ is based on $c = 6$. Figure 8 shows the slow convergence of the estimated value $\hat{\tau}_{\text{int},|\mathscr{M}|}$ toward its final value.

We compare these results with those obtained by Wolff's scheme (46), (48). As Fig. 8 shows, the estimate $\hat{\tau}^{\text{W}}_{\text{int},|\mathscr{M}|}$ of Wolff converges much faster than $\hat{\tau}^{\text{MS}}_{\text{int},|\mathscr{M}|}$. As expected, both estimates agree, the latter being always smaller than the first due to a residual bias. The fast convergence does not imply that the estimate $\hat{\tau}^{\text{W}}_{\text{int},|\mathscr{M}|}$ is better than $\hat{\tau}^{\text{MS}}_{\text{int},|\mathscr{M}|}$: in any case one has to analyze the convergence of $\hat{\tau}^{\text{W}}_{\text{int},|\mathscr{M}|}$ for large parameters c. Otherwise, one might erroneously extrapolate *apparently* asymptotic behavior to a wrong estimate. In our analysis, we calculate $\hat{\tau}^{\text{W}}_{\text{int},|\mathscr{M}|}$ in the interval $c \in [0, 6]$ and average over the interval $c \in [3, 6]$, where we find no systematic trends. The resulting estimates of $\tau_{\text{int},\mathscr{A}}$ for our three observables are summarized in Table III. The errors of $\hat{\tau}_{\text{int},\mathscr{A}}$ have been calculated from averaging over

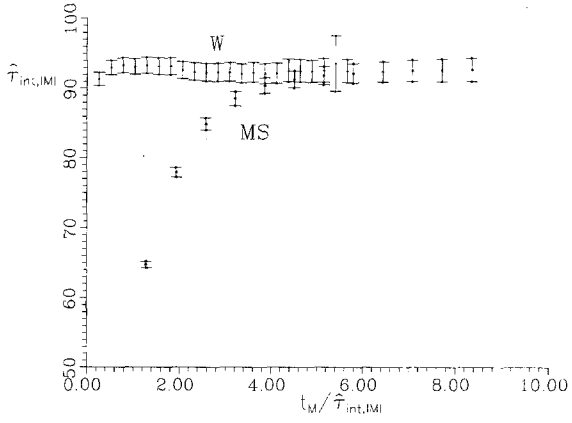

Fig. 8. Estimates of the integrated relaxation time $\tau_{\text{int},|\mathscr{M}|}$ calculated from a single run of a 36^3 lattice. $t_{\mathscr{M}}$ is identical to the cutoff parameter n_0 of (46). W refers to Wolff's method (48) and MS to the method of Madras and Sokal $[R(n_0) \equiv 0]$. Our final values and errors of $\hat{\tau}_{\text{int}}$ (Table III) have been averaged over the ensemble of simulations (Table I).

Table III. Summary of Exponential and Integrated Relaxation Times for the Observables $|\mathcal{M}|$, $\mathcal{E}$, and $\mathcal{M}$[a]

L	$\tau_{\exp,\lvert\mathcal{M}\rvert}$	$\tau_{\exp,\mathcal{E}}$	$\tau_{\exp,\mathcal{M}}$	$\tau_{\mathrm{int},\lvert\mathcal{M}\rvert}$	$\tau_{\mathrm{int},\mathcal{E}}$	$\tau_{\mathrm{int},\mathcal{M}}$
20	28.3 ± 0.2	28.0 ± 0.6	178.6 ± 1.1	27.3 ± 0.2	17.7 ± 0.2	173 ± 3
26	49.4 ± 0.3	49.7 ± 0.6	317.5 ± 5.0	47.4 ± 0.4	29.2 ± 0.2	306 ± 5
30	66.6 ± 0.3	67.7 ± 1.0	446 ± 7	62.7 ± 0.5	37.6 ± 0.3	424 ± 4
36	96.8 ± 0.7	94.3 ± 1.0	629 ± 11	93.3 ± 0.7	53.7 ± 0.5	596 ± 10
40	121.4 ± 0.4	128.6 ± 2.0	802 ± 11	116.0 ± 0.9	67.5 ± 0.5	733 ± 14
46	165 ± 2.0	160 ± 3.0	1005 ± 12	157.0 ± 1.5	87.6 ± 1.0	991 ± 21
50	195 ± 1.5	195 ± 2.0	1232 ± 43	186.0 ± 2.0	104.0 ± 1.5	1158 ± 30
60	278 ± 4.0	265 ± 6.0	1757 ± 43	271.0 ± 3.2	147.0 ± 2.2	1669 ± 47

[a] The statistical errors have been calculated from the variance over the ensemble of runs for each lattice size L. The data for integrated relaxation times refer to the estimation via Wolff's method [Eqs. (46) and (48)]. The estimate using the scheme of Madras and Sokal is always below but clearly within the error bars.

independent simulations of the same length (Table I). The comparison shows that energy correlations decay by a factor 1.8 faster than correlations of $|\mathcal{M}|$. This means that the tail of the spectrum $\rho_{\mathcal{E}}(\tau)$ of (13) carries more weight than that of $\rho_{|\mathcal{M}|}(\tau)$. Correlations of the odd observable $\mathcal{M}$ decay more slowly by a factor six. Fortunately, the latter are irrelevant for the statistical errors of thermodynamic properties.[22]

The determination of exponential relaxation times proceeds in the way sketched in Section 4. We perform exponential fits of our correlation function estimates $\hat{\Phi}(t)$ with amplitude and relaxation time as free parameters. Figure 1 (with a better time resolution) shows that $\mathcal{M}$ and $|\mathcal{M}|$ seem to follow asymptotic behavior below $\Phi \simeq 0.5$. Energy correlations are stronger influenced by short relaxation times; our initial estimate for the asymptotic time interval is $\Phi_{\mathcal{E}} < 0.3$. With $\tau_{\mathrm{int},\mathcal{A}}$ (Table III) and our trial value $\tau_{\exp,\mathcal{A}}$ for each observable, we calculate the power spectral density $P(\omega)$ in the approximation (44), which is compared to our estimate $\hat{P}(\omega)$. We find that deviations occur for $\mathcal{M}$ and $|\mathcal{M}|$ correlations only above $\Phi \simeq 0.6$. In contrast, energy correlations reach their asymptotic behavior in the interval $\Phi_{\mathcal{E}} < 0.1$, which is unexpectedly low. A fit of energy correlations outside this interval leads to a systematic underestimation of $\tau_{\exp,\mathcal{E}}$. Our final estimates of all exponential relaxation times determined in the asymptotic interval are contained in Table III. Errors are estimated from the average over our small ensemble of runs (Table I).

Critical exponents $z_{\exp,\mathcal{A}}$ and $z_{\mathrm{int},\mathcal{A}}$ are obtained by least-square fits of the relaxation times to the expected power laws (15) and (19). We find very good power-law behavior of $\tau_{\exp,\mathcal{A}}$ and $\tau_{\mathrm{int},\mathcal{A}}$ (Fig. 9). Fits have been

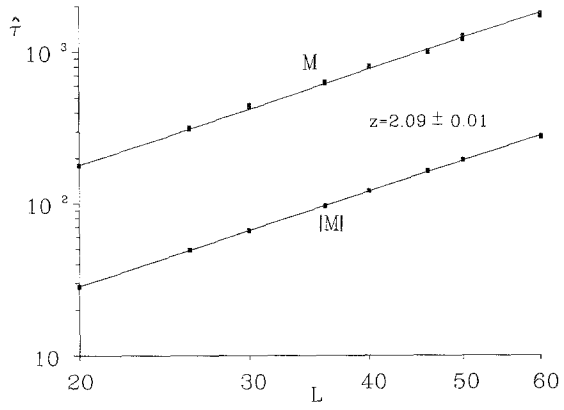

Fig. 9. Double logarithmic plot of power-law fits of exponential relaxation times $\hat{\tau}_{\exp,\mathcal{M}}$ and $\hat{\tau}_{\exp,|\mathcal{M}|}$. The symbol size is given by the error of the data (Table III). We find equal exponents $z_{\exp} = 2.09 \pm 0.01$ and a ratio $A_{\mathcal{M}}/A_{|\mathcal{M}|} = 6.2$.

performed with error weights (I) and with equal weights (II) for all lattice sizes. Comparison of our results I and II in Table IV indicates slightly smaller values for $z_{\exp}$ when calculated with equal relative weights. Our results for z_{int} are independent of the weighting method. Table IV contains the nonuniversal amplitudes as well. We verify that even observables have the same amplitude: $A_{\mathcal{E}} \simeq A_{|\mathcal{M}|}$. The scaling function of the ratio $\tau_{\exp,\text{odd}}/\tau_{\exp,\text{even}}$, Eq. (45), is $f(L/\xi) = 6.2$ in the finite-size limit $L/\xi \to 0$. Additional simulations with less accuracy in the bulk limit $L/\xi \gg 1$ are depicted in Fig. 10. They lead to comparable values for z and to

Table IV. Dynamical Critical Exponents $z_{\exp}$ and z_{int} Obtained from Error-Weighted (I) and Unweighted (II) Fits to Power-Law Behavior $\tau = AL^z$ [a]

	$\lvert\mathcal{M}\rvert$	$\mathcal{E}$	$\mathcal{M}$
$z_{\exp}^{(\text{I})}$	2.09 ± 0.01	2.10 ± 0.03	2.09 ± 0.04
$A_{\exp}^{(\text{I})}$	0.053	0.055	0.33
$z_{\exp}^{(\text{II})}$	2.09 ± 0.01	2.07 ± 0.03	2.07 ± 0.04
$A_{\exp}^{(\text{II})}$	0.054	0.059	0.38
$z_{\text{int}}^{(\text{I})}$	2.095 ± 0.008	1.94 ± 0.02	2.05 ± 0.04
$A_{\text{int}}^{(\text{I})}$	0.051	0.053	0.39
$z_{\text{int}}^{(\text{II})}$	2.096 ± 0.008	1.94 ± 0.02	2.05 ± 0.02
$A_{\text{int}}^{(\text{II})}$	0.051	0.053	0.38

[a] The main result in the first line shows convincingly clearly that odd and even observables have the same dynamical exponent z. For further discussion see the text.

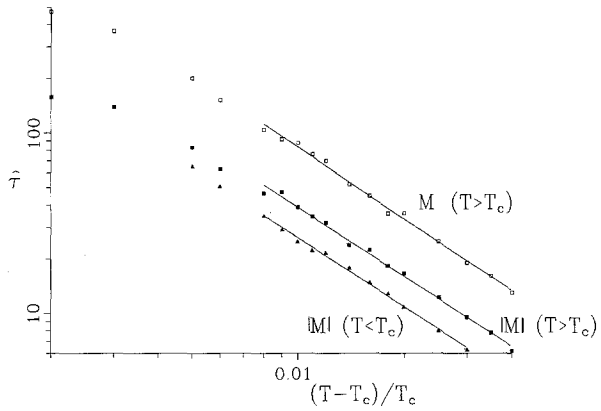

Fig. 10. The fit of $\hat{\tau}_{\exp,\mathscr{A}}$ to the power law $\tau_{\exp,\mathscr{A}} = A\,|\varepsilon|^{-\nu z}$ in the bulk regime $L/\xi \gg 1$ leads to the exponent $z = 2.06 \pm 0.03$ for the observables $\mathscr{M}$ and $|\mathscr{M}|$. The amplitude ratio $A_{\mathscr{M}}/A_{|\mathscr{M}|}$ well above T_c is 2.0. One can observe the increase of this ratio as T_c is approached from above. Below T_c we have studied $|\mathscr{M}|$ only; the exponential divergence of $\tau_{\exp,\mathscr{M}}$ and its crossover to power-law behavior at T_c has not been studied.

$f(L/\xi) \simeq 2.0$ for $L/\xi \to \infty$. This change of the scaling function f with L/ξ is schematically depicted in Fig. 5.

Our summary of z values (Table IV) contains some surprising results. As expected from universality, all three observables scale with the same exponent $z_{\exp} = 2.09 \pm 0.02$ within the errors, but this exponent is clearly larger than the renormalization group result $z \simeq 2.02$. A similarly interesting result is that the critical exponents $z_{\text{int},\mathscr{M}}$ and $z_{\text{int},|\mathscr{M}|}$ of integrated relaxation times agree with the asymptotic exponent $z_{\exp}$ within the errors. From the initial time dependence of the correlation functions of these observables in the interval $\Phi_{\mathscr{A}} \leqslant 0.5$ we infer that time scales shorter than $\tau_{\exp,\mathscr{A}}$ have to be included in a valid description [Eq. (13)] of correlations. Thus, there is a small deviation of the measure $\rho_{\mathscr{A}}(\tau)$ from a δ-like measure $\delta(\tau - \tau_{\exp,\mathscr{A}}(L))$. The agreement of exponential and integrated exponents within the errors may indicate that shorter relaxation modes scale with the same exponent as $\tau_{\exp,\mathscr{A}}$. But since the overlap with slower modes is small, this interpretation cannot be proven by our results. It is just one possibility to explain our findings. It might as well be possible that within our errors $z_{\text{int},\mathscr{A}}$ is smaller than but very near $z_{\exp}$, allowing for a different scaling behavior of the next-to-leading time scales. This is still an open question. In view of the finite-size scaling corrections to be discussed below, a clarification of these "fine-structure" effects is highly difficult.

The difference between $z_{\text{int},\mathscr{E}}$ and $z_{\exp,\mathscr{E}}$ definitely exceeds the error. This result is in good accord with the initial relaxation of energy correla-

tions in the interval $\Phi_{\mathscr{A}}(t) \geqslant 0.1$. We must conclude that next-to-leading relaxation times are not negligible and that they scale in a different way than the exponential relaxation time $\tau_{\exp,\mathscr{E}}$.

From the theoretical point of view, the discrepancy of the dynamical exponent z from its RG value is very important. In view of the small statistical errors the deviation is worrying. The error of the RG estimate for

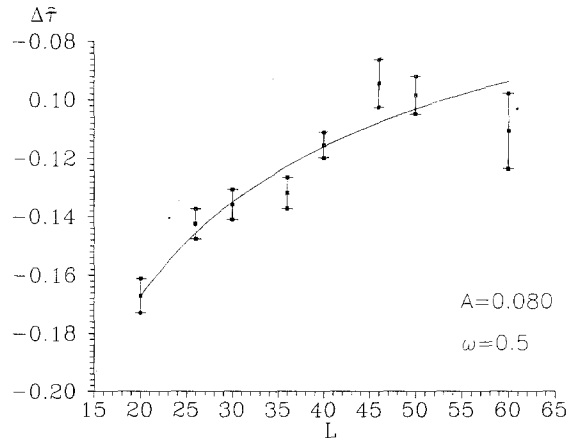

(a)

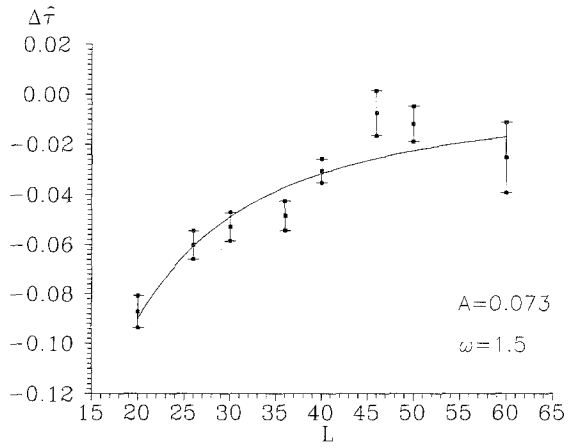

(b)

Fig. 11. Deviations from the expected theoretical behavior described by $z_{\text{th}} = 2.02$. We have fitted $\Delta\hat{\tau}_{\exp,|\mathscr{A}|} \equiv \hat{\tau}_{\exp,|\mathscr{A}|}/AL^{z_{\text{th}}} - 1$, i.e., the scaling correction of Eq. (50) to our data, keeping $z_{\text{th}} = 2.02$ fixed. One obtains fits with comparable estimators for a large set of parameters A, B, and ω. The figure shows that scaling corrections must be at least of the order of 10% if $z_{\text{th}} = 2.02$ is assumed to be correct.

$d = 3$ dimensions is not known, but the smallness of fluctuation corrections in $O(\varepsilon^2)$ gives no reason to expect that a higher-order expansion in ε will lead to significant changes.

We have so far ignored finite-size corrections completely. In static quantities, one observes a 1% deviation of exponents like γ/ν when fitting the susceptibility to simple power laws in a lattice interval $L \in [20, 60]$.[16] This has been tested by our own static susceptibility data. Dynamic finite-size effects must be much larger if they are responsible for the discrepancy of our estimated value of z from the theoretical value. To test this idea, we fit our most accurate data, the relaxation times $\tau_{\exp,|\mathscr{M}|}$ (Table III), to the ansatz

$$\tau_{\exp,|\mathscr{M}|} = AL^{z_{\text{th}}}(1 + BL^{-\omega}) \tag{50}$$

assuming the theoretical exponent $z_{\text{th}} = 2.02$ to be correct. With A, B, and ω as free parameters, we find equally good fits for a large, continuous set of parameters. As Fig. 11 shows, it is impossible to get a unique estimate of the correct finite-size scaling parameters. However, it is obvious from the fits that finite-size effects must be of the order of 10% if $z_{\text{th}} = 2.02$ is asymptotically valid.

7. DERIVATION OF z BY A SCALING METHOD

The numerical coincidence of $z_{\exp,\mathscr{A}}$ and $z_{\text{int},\mathscr{A}}$ for both observables $\mathscr{M}$ and $|\mathscr{M}|$ within our errors leads to the idea that if the integral $\tau_{\text{int},\mathscr{A}}$ in (16) over the spectrum (13) scales with the same exponent as its suprenum $\tau_{\exp,\mathscr{A}}$, then the whole or most of the spectrum $\rho_{\mathscr{A}}(\tau)$ possibly scales in this way. This hypothesis can be tested by analysis of the scaling properties (34) of the correlation functions. We assume mere scaling

$$\Phi_{\mathscr{A}}(t, L) = \Phi_0(tL^{-z}) \tag{51}$$

i.e., we make no assumption about the scaling function $\Phi_0(x)$ itself. This minimal ansatz has the merit of yielding z in those cases where scaling is valid, but the explicit functional form of $\Phi_0(x)$ is not known. Moreover, the comparison of data errors and fit errors allows a determination of the data interval where scaling is fulfilled.

Our scaling method works as follows. For each lattice size ν ($\nu = 1,..., \kappa$), we have $m(\nu)$ correlation function estimates $\{\hat{\Phi}(t_1),..., \hat{\Phi}(t_{m(\nu)})\}$. We have arranged the distance between measurements such that $m(\nu) =$ 100–250. In order sensibly to apply the scaling method, one should collect an equal amount of data for all lattices in the interval $[x_a, x_b]$ where scaling

is expected. An approximate value for z is therefore desirable. The usual fitting procedure[46] is to minimize the weighted estimator

$$Q = \sum_{\nu=1}^{\kappa} \sum_{t=t_1}^{t_{m(\nu)}} \frac{[\hat{\Phi}(t, L_\nu) - \Phi_0(tL_\nu^{-z})]^2}{\mathrm{var}(\hat{\Phi}(t, L_\nu))} \tag{52}$$

by appropriately chosen parameters of the function $\Phi_0(x)$ and z, respectively. The denominator is the estimated variance of $\hat{\Phi}(t, L_\nu)$, (27).

In order to design a "fitting procedure" to an unknown scaling function $\Phi_0(x)$ it is sensible to formulate the estimator Q of (52) in the inverse way. We assume that $\Phi_0(x)$ has an inverse $\Phi_0^{(-1)}(x)$, so that $t_0(x, L_\nu) \equiv L_\nu^z \Phi_0^{(-1)}(x)$ for each L_ν. An estimator equivalent to Q of (52) is then given by

$$Q = \sum_{\nu=1}^{\kappa} \sum_{\Phi=\Phi_1}^{\Phi_{m(\nu)}} \frac{[\hat{t}(\Phi, L_\nu) - t_0(tL_\nu^{-z}, L_\nu)]^2}{\mathrm{var}(\hat{t}(\Phi, L_\nu))} \tag{53}$$

where we assume Φ to be the argument and the corresponding time $\hat{t}$ to be the estimated quantity with variance $\mathrm{var}(\hat{t}(\Phi, L)) = \mathrm{var}(\hat{\Phi})/\Phi'^2(t, L)$. Here Φ' is the derivative with respect to the time t.

Applying the scaling method to an *unknown* function $\Phi_0(x)$, we minimize the weighted deviation of all pairs of the set $\{\hat{\Phi}(\{t\}, L_\nu)\}$ and $\{\hat{t}(\{\Phi\}, L_\nu)\}$, respectively, from one another:

$$\tilde{Q} = \frac{1}{N_p} \sum_{\substack{\nu,\mu=1 \\ \nu<\mu}}^{\kappa} \sum_{\Phi=\Phi_1}^{\Phi_{m(\nu)}} \frac{[\hat{t}(\Phi, L_\mu) - \hat{t}(\Phi, L_\nu)]^2}{[\mathrm{var}(\hat{t}(\Phi, L_\mu))\,\mathrm{var}(\hat{t}(\Phi, L_\nu))]^{1/2}} \tag{54}$$

The estimator $\tilde{Q}$ is normalized to the number N_p of lattice pairs. Since we have only a discrete set of data points $\{(t_1, \Phi(t_1)), \ldots, (t_{m(\nu)}, \Phi_{m(\nu)})\}$ for each lattice size L_ν, we proceed as follows: for each data point Φ of lattice L_ν we look up the corresponding time $\hat{t}(\Phi, L_\nu)$ in the data records. The corresponding time $\hat{t}(\Phi, L_\mu)$ of lattice L_μ which has the same value of Φ is calculated by linear interpolation of the data. To this end, data points should be close to one another.

This method works excellently if only one parameter is to be estimated (here z) by the data collapse. If there are two or more parameters as in a data collapse of unnormalized correlation functions $\phi(t, L)$ (here z and γ/ν are free parameters), a unique determination of the parameters is impossible.

We apply the method to our best correlation estimates $\hat{\Phi}_{|\mathscr{M}|}(t)$ using the complete set of lattice sizes $L \in [20, 60]$ but different intervals of the scaling variable $x = tL^{-z}$. In the initial relaxation phase $\Phi \in [0.9, 0.6]$, the best collapse is obtained for $z_{\mathrm{scal}, |\mathscr{M}|} = 2.05 \pm 0.02$, but with a normalized estimator $\tilde{Q} \simeq 18$.[54] In the interval $\Phi \in [0.6, 0.1]$ we find the exponent

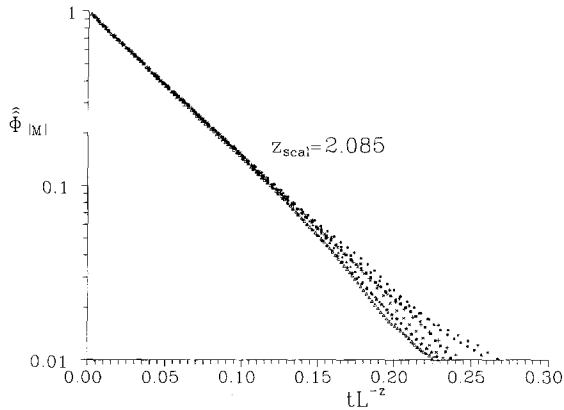

Fig. 12. The data collapse of $\hat{\Phi}_{|\mathcal{M}|}(t, L)$ leads to good scaling behavior in the interval $\Phi \in [0.6, 0.1]$. The deviation from scaling behavior in the initial relaxation phase $\Phi \in [0.9, 0.6]$ is not visible within the resolution of the figure. The scatter of the data below $\Phi \simeq 0.1$ is purely statistical (see Fig. 2).

$z_{\text{scal},|\mathcal{M}|} = 2.085 \pm 0.01$ and an estimator $\tilde{Q} \simeq 2.6$ (Fig. 12). Since a value $\tilde{Q} \simeq 1$ should be found if scaling is fulfilled within the statistical errors of the data, we conclude that the initial relaxation phase does not fulfill scaling to the expected accuracy. The average deviation in the interval $\Phi \in [0.9, 0.6]$ is a factor four times larger than the statistical errors of the data. In the interval $\Phi \in [0.6, 0.1]$, which is within our asymptotic time regime according to our analysis (Section 6), the data fulfill scaling very well. The exponent $z_{\text{scal},|\mathcal{M}|} = 2.085 \pm 0.01$ does not change upon variation of the Φ interval. $z_{\text{scal},|\mathcal{M}|}$ is in excellent agreement with our estimates $z_{\text{exp},|\mathcal{M}|} = 2.09 \pm 0.01$ and $z_{\text{int},|\mathcal{M}|} = 2.095 \pm 0.008$.

The numerical agreement of these exponents is now well understood: if scaling of $\Phi(t, L)$ is fulfilled with the exponent $z_{\text{scal},|\mathcal{M}|} \simeq z_{\text{exp},|\mathcal{M}|}$ in different intervals, then the integral $\tau_{\text{int},\mathcal{M}}$ over $\Phi_{|\mathcal{M}|}(t)$ must scale as well with the same exponent $z_{\text{int},|\mathcal{M}|}$. The scaling method is naturally more sensible to a variation of the exponent z_{scal} with the scaling interval than the analysis of the integrated relaxation time. This is clear since τ_{int} is an average over the *whole* spectrum, whereas the scaling method allows one to test scaling in separate intervals. In our case, the deviation of $z_{\text{scal},|\mathcal{M}|}$ in the initial interval $\Phi \in [0.9, 0.6]$ from the asymptotic value $z_{\text{scal},|\mathcal{M}|} = 2.085 \pm 0.01$ is pretty small, so that the difference is not detectable in the scaling analysis of $\tau_{\text{int},|\mathcal{M}|}$ (Section 6).

The scaling analysis of energy correlations shows that there are large nonscaling contributions to $\Phi_{\mathcal{E}}(t)$. These contributions are expected because the specific heat $C \sim L^d \phi_{\mathcal{E}}(t=0)$ contains large nonsingular contributions.[47] Our scaling analysis is inappropriate in this case because

more parameters would have to be determined. However, the bad scaling properties of $\Phi_{\mathscr{E}}(t, L)$ explain the unusual exponent $z_{\text{int},\mathscr{E}}$ found from the scaling of $\tau_{\text{int},\mathscr{E}}$ in Section 6. Large contributions to $\Phi_{\mathscr{E}}(t)$ by smaller relaxation times $\tau < \tau_{\text{exp}}$ are important for the energy. These contributions scale in a different way and lead to smaller effective values of $\tau_{\text{int},\mathscr{E}}$, Eq. (16).

8. OUTLOOK

We have presented a large-scale simulation about the dynamical critical behavior of the three-dimensional Ising model. As one of the standard model systems in statistical physics, its understanding is of vital importance for further progress in the field of dynamic critical phenomena. It is generally expected that the dynamic renormalization group is a sound description. We believe that the disagreement of renormalization group results and Monte Carlo simulations originates from technical problems.

On the side of the renormalization group, the hardest technical obstacle for a reliable dynamic exponent z in $d=3$ dimensions is the extrapolation and resummation, respectively, of perturbation analysis. Until now, the renormalization group has been calculated to second order in $\varepsilon = 4 - d$ and in an expansion around dimension $d=1$. The numerical interpolation between these expansions is not well founded. A significant improvement could be obtained by an application of the renormalization group in fixed dimension.[48] Similar to static critical phenomena, irrelevant operators should be included into the formalism in order to obtain Wegner corrections[49] for dynamic critical phenomena. Finally, a (finite-size) scaling analysis of the relevant part of the spectrum of the Liouville operator would be most welcome.

Monte Carlo work is inherently confronted with technical problems induced by random number generation, the finite size of the system, finite length of simulations, etc. In view of these aspects, it is not expected that a single simulation will clarify the situation and yield a reliable value of the dynamic exponent. In order to eliminate technical obstacles, the simulation and analysis should be performed with different random number generators, dynamics, system sizes, and boundary conditions. The large-scale simulation presented here is a part of the puzzle.

However, we have also presented a systematic approach to the determination of exponential relaxation times. These time scales are crucial for the comparison with theory as long as theory can only deal with asymptotic behavior. The use of the power spectral density for the long-time analysis of the dynamics is new. The great error reduction compared to correlation function estimates shows that it is convincing tool. The agreement of our numerical estimates of $z_{\text{exp},\mathscr{A}}$ and $z_{\text{int},\mathscr{A}}$ for both $\mathscr{A} = \mathscr{M}$ and $\mathscr{A} = |\mathscr{M}|$

within the statistical errors is a surprising result. For energy correlations, $z_{\exp,\mathscr{E}}$ and $z_{\text{int},\mathscr{E}}$ differ significantly. Both results are substantially confirmed by the scaling analysis in the last section. However, in view of significant finite-size scaling corrections, we cannot make strong statements about an exact equality or inequality of integrated and exponential exponents and about the scaling behavior of next-to-leading relaxation times.

The dynamic exponent $z = 2.09 \pm 0.02$ has to be viewed with the same care as the interpolation of renormalization group results to dimension $d = 3$. We need a closer look at dynamic finite-size corrections, which have been ignored completely in earlier work. An extension of the present work to larger lattices but with the same accuracy is necessary to achieve this aim.

APPENDIX

In this Appendix we provide a short summary of the estimation of frequency-dependent properties in time series analysis[36] which is indispensable for the analysis of Monte Carlo simulations.

The estimator $I_n^*(\omega)$ in (30) of the power spectral density provides an instructive example that a *natural* estimator may be statistically useless. The reason for the failure of I_n^* becomes apparent from Eq. (29), which is a sum over n sample autocovariances $\hat{\Phi}(t)$, each of which has a variance of $O(1/n)$.[36] Thus, I_n^*, Eq. (29), has a variance of $O(1)$ and is not a consistent estimator of $P(\omega)$, Eq. (20). Note that this argument is not affected by the correlation (26) of the $\hat{\phi}(t)$ for different times. One may say that the tail of the sum $I_n^*(\omega)$ in (29) contains only noise but no information, so that the good statistics contained in the initial terms of the sum is lost in the noise of the tail. The remedy is to cut off the sum in an appropriate way so that the noise is lost but the valuable information is retained.

This problem and its solution for the integrated relaxation time $\tau_{\text{int}} = \pi P(0)$ have been discussed by Madras and Sokal[33] and in a modified way by Wolff.[41] The obvious solution is to truncate I_n^* of (29) at some n_0 and neglect the tail. This defines the truncated sample spectral density function[36]

$$\hat{P}_n(\omega) = \frac{1}{2\pi} \sum_{t=-n_0}^{n_0} \hat{\phi}(t) \cos \omega t \tag{A1}$$

which has a variance $\text{var}(\hat{P}_n)(\omega) = O(n_0/n)$.[36] In the limit of infinite record length n the variance vanishes as

$$\text{var}(\hat{P}_n(\omega)) \to 0 \qquad \left(n, n_0 \to \infty; \frac{n_0}{n} \to 0\right) \tag{A2}$$

However, the truncation induces a bias, so that the estimator (A1) is only asymptotically unbiased. The idea to truncate the sum (29) is generalized to smooth cutoffs by other lag windows $\{\lambda_n(t)\}$ in the following way:

$$\hat{P}_n(\omega) = \frac{1}{2\pi} \sum_{t=-(n-1)}^{(n-1)} \lambda_n(t)\, \hat{\phi}(t) \cos \omega t \tag{A3}$$

A variety of lag windows are commonly used in time series analysis.[36] They all have in common that their initial part has full weight and decreases to zero for longer times in their characteristic way.

It is favorable to introduce the spectral window which is the Fourier transform of the lag window:

$$W_n(\theta) = \frac{1}{2\pi} \sum_{t=-(n-1)}^{(n-1)} \lambda_n(t) \exp(-i\theta t) \tag{A4}$$

Then the estimator $\hat{P}_n(\omega)$ is an integral over the frequency interval $[-\pi, +\pi]$:

$$\hat{P}_n(\omega) = \int_{-\pi}^{+\pi} I_n^*(\theta)\, W_n(\omega - \theta)\, d\theta \tag{A5}$$

Written in this way, the estimator $\hat{P}_n(\omega)$ is a locally weighted sample spectral density function whose values are weighted averages over small intervals in the frequency domain. The form of the spectral window $W_n(\theta)$ is related to the lag window: the more slowly $\lambda_n(t)$ decays to zero, the more concentrated is its spectral window $W_n(\theta)$. The bias $b(\omega) \equiv [\hat{P}_n(\omega)] - P(\omega)$ induced by the window for a finite time series is given by[36]

$$b(\omega) \sim \tfrac{1}{2} P''(\omega) \int_{-\pi}^{\pi} \theta^2 W_n(\theta)\, d\theta \tag{A6}$$

The bias depends on the width of the spectral window and on the curvature of the spectral density $P(\omega)$. One may tailor the form of the spectral window to the spectral density in order to obtain best-adapted windows for each case. The variance of the estimate (A5) is given by

$$\mathrm{var}(\hat{P}_n(\omega)) \simeq (1 + \delta_{\omega,0,\pi})\, P^2(\omega) \frac{2\pi}{n} \int_{-\pi}^{\pi} W_n^2(\theta)\, d\theta \tag{A7}$$

which may also be written as a sum over times as

$$\mathrm{var}(\hat{P}_n(\omega)) \simeq (1 + \delta_{\omega,0,\pi})\, P^2(\omega) \frac{1}{n} \sum_{-(n-1)}^{n-1} \lambda_n^2(t)\, dt \tag{A8}$$

We argued in Section 3 that the covariance of the periodogram I_n of (29) calculated from a finite record length vanishes, leading to wildly fluctuating estimators $I_n(\omega)$. The covariance of the spectral estimate $\hat{P}(\omega)$ of (A1) is given by[36]

$$\operatorname{cov}(\hat{P}_n(\omega_1), \hat{P}_n(\omega_2)) \simeq \frac{2\pi}{n} \int_{-\pi}^{\pi} P^2(\theta)\, W_n(\omega_1 - \theta)\, W_n(\omega_2 - \theta)\, d\theta \quad \text{(A9)}$$

As expected, it vanishes only in the limit of an infinite record length, since $\hat{P}_n(\omega_1)$ and $\hat{P}_n(\omega_2)$ are asymptotically uncorrelated. In a finite time series, the covariance is restored by the weighting procedure, so that one obtains a smooth sequence $\{\hat{P}_n(\omega)\}$ of data points.

Finally, we mention some explicit results for the Daniell window used in this paper. The Daniell window performs an average of the periodogram data $\hat{I}_n^*(\omega)$ over small frequency intervals. It is defined by

$$W_n(\theta) = \begin{cases} n_0/2\pi & \text{for} \quad |\theta| \leqslant \pi/n_0 \\ 0 & \text{otherwise} \end{cases} \quad \text{(A10)}$$

From the result for the covariance (A9), one realizes that the estimators at two frequencies ω_1 and ω_2 are effectively uncorrelated if $|\omega_1 - \omega_2| > 2\pi/n_0$. The variance of the Daniell window estimates follows from (A7) as

$$\operatorname{var}(\hat{P}_n(\omega)) \simeq \frac{n_0}{n} P^2(\omega) \qquad (\omega \neq 0, \pm\pi) \quad \text{(A11)}$$

which agrees with previous considerations of the truncated sample spectral density (A1). The bias $b(\omega)$ of the Daniell window estimate follows from (A6) as

$$b(\omega) \simeq \frac{\pi^2}{6n_0^2} P''(\omega) \quad \text{(A12)}$$

Similar results with different numerical factors may be calculated for other windows; they are summarized in ref. 36.

There is no unique answer to the question of what are the best choices of the record length n, the type of window, and its parameter n_0. They depend on the spectral density to be estimated, on the frequency interval, on the desired resolution, and on other aspects discussed in the literature.[36]

We apply the results summarized above to the analysis of Monte Carlo simulations. In the general case, one may vary the record length n and choose a certain spectral window and its window parameter n_0. Here,

we assume a fixed record length n and we assume that one is interested in the complete functional dependence $P(\omega)$ of the power spectral density in some frequency interval. As discussed above, one has to compromise between bias and variance. This is accomplished by minimizing the relative mean square error

$$\eta^2(\omega) = \frac{\mathrm{var}(\hat{P})}{P^2} + \frac{b^2}{P^2} \tag{A13}$$

$$= \alpha \frac{n_0}{n} + \beta \frac{1}{n_0} \left| \frac{P''(\omega)}{P(\omega)} \right|^2 \tag{A14}$$

where α and β are numerical factors characteristic of the chosen window [$\alpha = 1$ and $\beta = \pi^4/36$ for the Daniell window (A11), (A12)]. The optimal choice of the window parameter n_0 follows as

$$n_0 = \left(\frac{4\beta}{\alpha} \right)^{1/5} \left| \frac{P''}{P} \right|^{2/5} n^{1/5} \tag{A15}$$

which depends on the curvature of the power spectral density at frequency ω. The resulting mean square error (A13) of $\hat{P}_n(\omega)$ is given by

$$\eta^2(\omega) = \frac{5\alpha}{4} \left(\frac{4\beta}{\alpha} \right)^{1/5} \left| \frac{P''(\omega)}{P(\omega)} \right|^{2/5} n^{-4/5} \tag{A16}$$

The squared bias contribution to η is 1/4 of the variance in this optimal solution. Equation (A16) shows that the mean square error of the spectral estimate $\hat{P}_n(\omega)$ of (A3) decreases as $n^{-4/5}$, so that it is a consistent and asymptotically unbiased estimate. The optimal solution n_0 of (A15) depends on the frequency ω via the bandwidth $B \equiv 2\,|P/P''|^{1/2}$ of the spectrum. One may either choose a frequency-dependent value of $n_0(\omega)$ in (A15) or simplify matters by taking the lower limit of the bandwidth over the whole interval to calculate a unique value of n_0. In the latter case, the mean square error $\eta^2(\omega)$ may be far from optimal in a large region of the frequency interval. As an example, we assume a simple exponential decay of correlations with a relaxation time τ. The bandwidth of its Lorentzian spectrum (39) near $\omega = 0$ is given by $B(\omega) = \sqrt{2}/\tau$. The optimal window parameter (A15) given by

$$\frac{n_0}{\tau} = \left(\frac{16\beta}{\alpha} \right)^{1/5} \left(\frac{n}{\tau} \right)^{1/5} \tag{A17}$$

depends on the number of effectively uncorrelated data. For the Daniell window, a typical value for a large-scale simulation with $n = 10^5\tau$ time

steps like the one presented in this paper is given by $n_0 = 21\tau$. This value refers to the vicinity of the interesting long-time behavior. For short times the bandwidth increases significantly, so that the bias (A6) is reduced even for smaller values of n_0. In our analysis we compromised between the above-mentioned alternatives and split the spectrum into a short- and a long-time regime with different values of n_0.

ACKNOWLEDGMENTS

The author thanks A. D. Sokal for numerous improvements of the original manuscript. His suggestions and comments have been worked into the present form of the paper.

This work was supported by the Sonderforschungsbereich SFB 166 "Disorder and Large Fluctuations." The author is grateful to the HLRZ/Jülich for computing time on the CRAY Y-MP 832.

REFERENCES

1. B. I. Halperin and P. C. Hohenberg, *Phys. Rev.* **117**:951 (1969).
2. P. C. Hohenberg and B. I. Halperin, *Rev. Mod. Phys.* **49**:435 (1977).
3. M. Suzuki, *Prog. Theor. Phys.* **58**:1141 (1977).
4. M. C. Yalabik and J. D. Gunton, *Prog. Theor. Phys.* **62**:1573 (1979).
5. A. D. Sokal, *Nucl. Phys. B (Proc. Suppl.)* **20**:55 (1991).
6. C. De Dominicis, E. Brezin, and J. Zinn-Justin, *Phys. Rev. B* **12**:4945 (1975).
7. J. C. LeGuillou and J. Zinn-Justin, *Phys. Rev. B* **21**:3976 (1980).
8. R. Bausch, V. Dohm, H. K. Janssen, and R. K. P. Zia, *Phys. Rev. Lett.* **47**:1837 (1981).
9. H. Yahata, *J. Phys. Soc. Jpn.* **30**:657 (1971).
10. Z. Alexandrowicz, *Physica A* **167**:322 (1990).
11. Z. Alexandrowicz, *Physica A* **189**:148 (1992).
12. C. M. Fortuin and P. W. Kasteleyn, *Physica* **57**:536 (1972).
13. B. K. Chakrabarti, H. G. Baumgärtel, and D. Stauffer, *Z. Phys. B* **44**:333 (1981).
14. N. Jan, L. L. Moseley, and D. Stauffer, *J. Stat. Phys.* **33**:1 (1983).
15. C. Kalle, *J. Phys. A* **17**:L801 (1984).
16. R. B. Pearson, J. L. Richardson, and D. Toussaint, *Phys. Rev. B* **31**:4472 (1985).
17. G. Parisi and F. Rapuano, *Phys. Lett.* **157B**:301 (1985).
18. G. Bhanot, D. Duke, and R. Salvador, *Phys. Rev. B* **33**:7841 (1986).
19. P. H. Poole and N. Jan, *J. Phys. A* **23**:L453 (1990).
20. S. Wansleben and D. P. Landau, *Phys. Rev. B* **43**:6006 (1991).
21. K. MacIsaac and N. Jan, *J. Phys. A* **25**:2139 (1992).
22. H.-O. Heuer, *J. Phys. A* **25**:L567 (1992).
23. D. Stauffer, *Physica A* **186**:197 (1992).
24. N. Ito, preprint (1992).
25. G. S. Pawley, R. H. Swendsen, D. J. Wallace, and K. G. Wilson, *Phys. Rev. B* **29**:4030 (1984).
26. H. W. J. Blöte *et al.*, *Physica A* **161**:1 (1989).
27. C. F. Baillie *et al.*, *Phys. Rev. B* **45**:10438 (1992).

28. J. Adler, *J. Phys. A* **16**:3585 (1983).
29. J. Q. Kemeny and J. L. Snell, *Finite Markov Chains* (Springer-Verlag, Berlin, 1976).
30. K. L. Chung, *Markov Chains with Stationary Transition Probabilities*, 2nd ed. (Springer-Verlag, Berlin, 1967).
31. E. Seneta, *Non-negative Matrices and Markov Chains*, 2nd ed. (Springer-Verlag, Berlin, 1981).
32. K. Binder, in *Phase Transitions and Critical Phenomena*, Vol. 5b, C. Domb and M. S. Green, eds. (Academic Press, 1976).
33. N. Madras and A. D. Sokal, *J. Stat. Phys.* **50**:109 (1988).
34. S. Kirkpatrick and E. P. Stoll, *J. Comp. Phys.* **40**:517 (1981).
35. H.-O. Heuer, *Physica A* **182**:649 (1992).
36. M. B. Priestley, *Spectral Analysis and Time Series*, Vol. 1 (Academic Press, 1981).
37. A. Beretti and A. D. Sokal, *J. Stat. Phys.* **40**:483 (1985).
38. Y. Y. Goldschmidt, *Nucl. Phys. B* **280**:340 (1987); **285**:519 (1987).
39. J. C. Niel and J. Zinn-Justin, *Nucl. Phys. B* **280**:355 (1987).
40. M. S. Bartlett, *J. Roy. Stat. Soc. Suppl.* **8**:27 (1946).
41. U. Wolff, *Phys. Lett. B* **228**:379 (1989).
42. J. C. Angles d'Auriac, R. Maynard, and R. Rammal, *J. Stat. Phys.* **28**:307 (1982).
43. A. M. Yaglom, *Correlation Theory of Stationary and Related Random Functions I and II* (Springer, 1987).
44. E. Stoll, K. Binder, and T. Schneider, *Phys. Rev. B* **8**:32661 (1973).
45. H. Meyer-Ortmanns and T. Trappenberg, *J. Stat. Phys.* **58**:185 (1990).
46. B. L. van der Waerden, *Mathematical Statistics* (Springer-Verlag, Berlin, 1969).
47. A. J. Liu and M. E. Fisher, *Physica A* **156**:35 (1989).
48. G. Parisi, *J. Stat. Phys.* **23**:49 (1980).
49. F. J. Wegner, *Phys. Rev. B* **5**:4529 (1972).